

**PRELIMINARY INDIAN OCEAN SKIPJACK TUNA STOCK
ASSESSMENT 1950-2019 (STOCK SYNTHESIS)**

PREPARED BY: DAN FU¹,

02 AUGUST 2020

¹ IOTC Secretariat, Dan.Fu@fao.org;

Contents

1. INTRODUCTION.....	4
1.1 Biology and stock structure.....	4
1.2 Fishery overview.....	5
2. OBSERVATIONS AND MODEL INPUTS.....	7
2.1 Spatial stratification	7
2.2 Temporal stratification.....	7
2.3 Definition of fisheries	8
2.4 Catch history	8
2.5 CPUE indices.....	9
2.5.1 Maldives PL CPUE series.....	9
2.5.2 EUROPEAN PSLs abundance indices series.....	9
2.5.3 EUROPEAN PSLs Echo Echosounder Buoys indices.....	9
2.5.4 Other abundance indices	9
2.6 Length frequency data.....	11
2.7 Tagging data.....	12
3. Model structural and assumptions	15
3.1 Population dynamics	15
3.1.1 Recruitment.....	16
3.1.2 Growth and Maturation.....	16
3.1.3 Natural mortality	17
3.2 Fishery dynamics	17
3.3 Dynamics of tagged fish	18
3.4 Modelling methods, parameters, and likelihood.....	18
3.5 Reference points.....	19
4. ASSESSMENT model runs.....	19
4.1 2017 model continuity run	19
4.2 Basic and sensitivity models	19
4.3 Final model assessable (grid).....	21
5. model RESULTS.....	22
5.1 2017 model continuity run	22
5.2 Basic models	23
5.2.1 Model fits.....	24
5.2.2 Model estimates	28
5.3 Sensitivity models.....	30
5.4 Final model options.....	32
5.5 Diagnostics.....	35
5.5.1 Profile likelihood.....	35
5.5.2 Retrospective analysis.....	36
5.5.3 Hindcasting analysis	37
6. Stock status.....	38
6.1 Current status and yields	38
7. DISCUSSION	40
8. ACKNOWLEDGMENTS	41
9. REFERENCES.....	42
APPENDIX A: FITS to length data for main fleets FROM THE basic model	46
Appendix B: SELECTED RESULTS FROM THE SENSIVITY MODELs.....	50
Appendix C: RUN TEST results FROM the TWO-AREA MODEL ‘io2’	56

SUMMARY

This report presents a preliminary stock assessment for Indian Ocean Skipjack tuna (*Katsuwona pelamis*) using *Stock Synthesis 3* (SS3). The assessment uses a spatially aggregated and seasonally structured model that integrates several sources of fisheries and biological data. An alternative, spatially explicit model is also considered in the final model assemble. The assessment model covers the period 1950–2019 and represents an update and revision of the 2017 assessment model with the inclusion of updated CPUE indices, and a revised fishery structure. A range of sensitivity models are presented to explore the impact of key data sets and model assumptions.

The assessment assumed the Indian Ocean skipjack tuna constitute a single spawning stock (the spatially disaggregated model partitions the stock into a western and eastern region). The assessment model defined 7 fisheries. Standardised CPUE series from Maldives Pole and line fleet 1995 – 2018 and EU associated Purse seine sets 1990 – 2019 were included in the models as relative abundance index of exploitable biomass. A newly available index based on acoustic data from echosounder buoys and an additional index based on associative dynamics of skipjack tuna with floating objects corroborate the recent trend of the Purse seine index, and the utility of these indices were examined in the assessment. Tag release and recovery data from the RTTP-IO program were included in the model to inform abundance and fishing mortality rates.

The final assessment model options correspond to a combination of model configurations, including alternative spatial structure (one-area or two-areas), alternative values of SRR steepness (0.7, 0.8, or 0.9), alternative tag mixing period (3 or 4 quarters), and the alternative values of tag weighting parameter ($\lambda = 1$ or 0.1). The model ensemble (a total of 24 models) encompass a range of stock trajectories. Estimates of stock status were combined across from the 24 models and incorporated uncertainty estimates from individual models as well as across the model ensemble.

IOTC Resolution 16/02 adopted a harvest control rule (HCR) for skipjack tuna, which recommends a annual catch limit based on a relationship between stock status (spawning biomass relative to unfished levels) and fishing intensity (exploitation rate relative to target exploitation rate), estimated from a model-based stock assessment. Therefore, this assessment reported depletion-based target reference points, including $SSB_{40\%}$ (40% of unfished spawning biomass), $F_{40\%SSB}$ (fishing mortality corresponding to 40% of the unfished spawning biomass), and the target yield (equilibrium catch at $F_{40\%SSB}$).

The overall stock status estimates do not differ substantially from the previous assessment. Biomass was estimated to have increased considerably from the historical low level in 2015. Spawning biomass in 2019 was estimated to be 45% of the unfished level. Current fishing mortality was estimated to be very close to $F_{40\%SSB}$ ($F_{2019} / F_{40\%SSB} = 0.98$). The probability of the stock being currently in the green Kobe quadrant is estimated to be 63%. Considering the quantified uncertainty, the stock is considered not to be overfished and is not subject to overfishing in 2019. The retrospective analysis provided some confidence on the robustness of the model with respect to recent data. However, the catches in the last two years have exceeded the catch limit set for 2018 – 2000 and are also higher than the estimated target yield ($Yield_{40\%SSB}$). The estimated stock status is summarized as below:

- Catch in 2019: 547 248
- Average catch 2015–2019: 506 554
- $Yield_{40\%SSB}$ (1000 t) (80% CI): 515 (445 –586)
- $F_{40\%SSB}$ 0.60 (0.53–0.66)
- SB_0 (1000 t) (80% CI): 1900 (1614–2191)
- SB_{2019} (1000 t) (80% CI): 854 (632–1077)
- $SB_{40\%SB0}$ 759 (641–877)
- $SB_{2019} / SB_{40\%SB0}$ 1.13 (0.98–1.28)
- $F_{2019} / F_{40\%SB0}$ 0.98 (0.75–1.21)

1. INTRODUCTION

The Indian Ocean skipjack tuna (*Katsuwona pelamis*, SKJ) fishery is one of the largest tuna fisheries in the world, with total catches of 400-600 thousand t over the past decade. Some bioeconomic modelling of the fish population and fishery was undertaken a few years ago (Mohamed 2007). Before 2010, management advice has relied on data-based indicators, and mortality estimates from analyses of the recent RTTP-IO tagging data (Edwards et al. 2010). A full integrated model-based assessment was developed in 2011 (Kolody 2011 et al), and further updated in 2012 (Sharma et al. 2012), 2014 (Sharma et al. 2014), and 2017 (Fu et al. 2017).

In 2016, the IOTC commission adopted a Harvest control rule (HCR) for the skipjack tuna through Resolution 16/02. The HCR shall recommend a total annual catch limit inferred from a relationship between stock status (spawning biomass relative to unfished levels) and fishing intensity (exploitation rate relative to target exploitation rate) estimated from a model-based stock assessment. The resolution also stated that the first implementation of the HCR would be based upon the 2017 skipjack stock assessment agreed by the WPTT19 and endorsed by the SC.

The assessment of skipjack tuna in 2017 implemented a range of exploratory models to explore the impact of key data and model assumptions (e.g. spatial and temporal structures) on the estimates of stock status. A systematic approach was undertaken to evaluate interactions of model assumptions and to develop management advice. Model options investigated in the exploratory phase were further refined during the WPTT19 which agreed upon a final assemble of 37 models to characterize key uncertainty (IOTC-2017-WPTT19). Subsequently, the SC applied the HCR to calculate the annual catch limit of skipjack tuna for the period 2018–2020, using the parameters estimated from the 2017 stock assessment model ensemble (Murua, et al. 2017).

The HCR described in Resolution 16/02 requests that the skipjack tuna stock assessment is conducted every three (3) years, with the next stock assessment scheduled in 2020. In this context, this report provides an update and further development of the integrated stock assessment for skipjack in the Indian Ocean. The model incorporates three additional years of data (2017–2019), improved information on nominal catches from IOTC database, and revised CPUE time series for the Maldives Pole and line and European Purse seine fleets. The assessment provides estimates of population parameters, stock status and reference quantities (required for the calculation of the catch limit from the HCR), with uncertainties characterised through a model grid running on combinations of model settings and parameter values. The assessment builds on the work by Fu (2017), Sharma et al. (2012, 2014), and Kolody (2011), and uses a size based, age structured population model, implemented in Stock Synthesis 3 (Methot and Wetzel 2013, Methot et al. 2020).

1.1 Biology and stock structure

Skipjack are the smallest of the major commercial tuna species and are found mainly in the tropical areas with geographic limits between 55-60° N and 45-50° S. Skipjack are highly fecund and can spawn year round over a wide area of the tropical and subtropical waters. Environmental conditions are believed to significantly influence recruitment and can produce widely varying recruitment levels between years (Mackenzie et al. 2016). The historical Japanese surveys of skipjack larvae have identified large quantities of skipjack larvae in the Equatorial Eastern IO (Nishikawa et al 1985), but these surveys have been quite rare in the Western IO. The location of skipjack nurseries remains widely unknown, as well as the biology of skipjack early juveniles, because very small sizes of skipjack have never been exploited significantly in the IO (Fonteneau 2014).

A substantial amount of information on skipjack movement is available from tagging programs, which have documented some large-scale movement within the Indian Ocean. The average range of movement during the skipjack lifetime can be estimated at about 1000 miles, with maximum distance of about

2000 miles (Fonteneau 2014). Skipjack movement is highly variable and is thought to be influenced by large-scale oceanographic variability (Mackenzie et al. 2016).

Genetic analyses by Dammannagado *et al.* (2011) have suggested that there might be two (or more) skipjack populations in the Indian Ocean. A recent stock structure study based on analysis of the shape of otolith from four areas south of Java showed that they are not statistically different among regions, suggesting that these skipjack belongs to a single stock (Wujdi et al. 2017). However, Due to the limited spatial range of the samples, this conclusion cannot be applied to the whole Indian Ocean. Using next generation genetic sequencing, Grewe (2019) suggested a weak genetic population differentiation of skipjack tuna from the central Indian Ocean through to the Eastern Pacific Ocean.

1.2 Fishery overview

The Indian Ocean skipjack catch history is shown in Figure 1. Catches increased steadily from the 1980s to a peak at over 600,000t in 2006, but have been decreasing since the mid-2000s. Since 2006 total catches have declined to around 340,000t in 2012 although since 2013 catches have increased sharply and in 2018 reached again a level of 600,000t mostly driven by the purse seine (associated school) fisheries. The catches in 2018 have exceeded the catch limit of 470, 000 t as set out by the skipjack Harvest Control Rule. Figure 2 illustrates the spatial distribution of the catches from the main fisheries (purse seine, pole and line, gillnet, line). In 2018, purse seine accounted for about 45% of the total catches, with the remainder of catches mainly taken by the gillnet (18%), pole and line (16%), and line (5%) fisheries. The catches in 2019 dropped slightly to about 550 000 t.

The Maldives has sustained a pole and line (PL, bait boat) skipjack fishery for many centuries, with catches increasing dramatically with the uptake of mechanization and deployment of larger vessels (more poles, larger bait and storage capacity, longer range) starting in the 1980s. The Maldives has experienced substantial catch declines since the peak in 2006, for reasons that are not entirely clear. Adam (2010) suggests that this may reflect declining skipjack abundance, limitations to bait availability or changing economic incentives (e.g. high fuel prices). In 2018 catches from this fishery reached again 100,000t, with most of these catches (over 80%) being caught in offshore waters (IOTC 2020).

There has been a rapid increase in skipjack catches with the introduction of the purse seine fleets in the 1980s, and the development of the fishery in association with Fish Aggregating Devices (FADs) since the 1980s (e.g. Chassot 2010, Delgado de Molina 2010). The European/Seychelles PS catch has fluctuated considerably since around 2000 without a clear trend. Catch declines in the recent years are probably partly attributable to the effects of piracy in the prime fishing area near Somalia. From 2003-06 the decline was due to very good fishing of large yellowfin tuna on free schools. After 2007 piracy or other ‘unknown’ reasons may be the cause of the decline. In recent years, well over 90% of the skipjack tuna caught by purse seine vessels are taken from around FADs.

Several fisheries using gillnets have reported large catches of skipjack tuna in the Indian Ocean, including the gillnet/longline fishery of Sri Lanka, driftnet fisheries of I.R. Iran and Pakistan, and gillnet fisheries of Indonesia. In recent years gillnet catches have represented as much as 20% to 30% of the total catches of skipjack tuna in the Indian Ocean. Although it is known that vessels from I.R. Iran and Sri Lanka have been using gillnets on the high seas in recent years, reaching as far as the Mozambique Channel, the activities of these fleets are not fully understood, as time-area catch-and-effort series have been made available for those fleets only in recent years (IOTC 2020). Moderate catches are taken by the line fishery representing a mixture of gears using handlines, trolling, and small longlines, mostly in the eastern Indian Ocean (Figure 2).

A substantial portion of the total catch is taken by a mix of artisanal gears, with minor catches dating back before the pre-industrial period. For the assessment, these fleets have been pooled together, in the heterogeneous *Other* fleet. The bulk of the recent catch in this fishery is from the small purse seiners fisheries of India, Indonesia, Malaysia, and Mozambique. These fleets were mostly operating in coastal waters. The aggregate catches of these fleets have been increasing more recently.

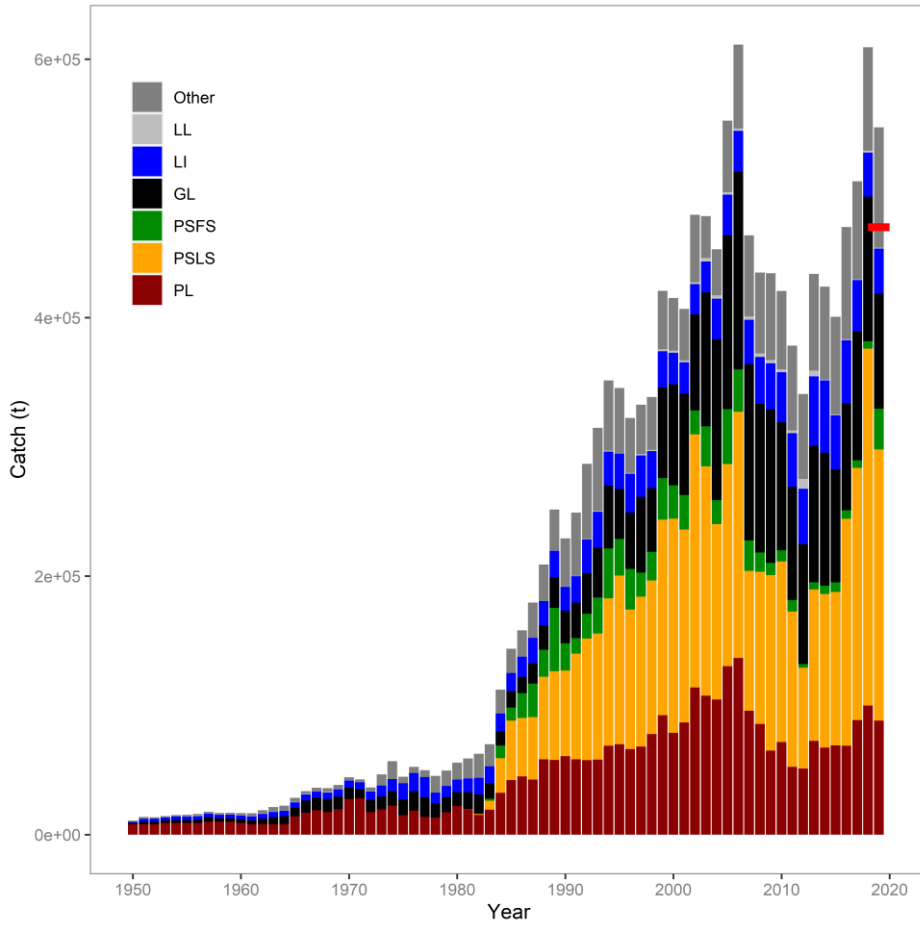


Figure 1: Total annual catch (1000s t) of skipjack tuna by fishery from 1950 to 2019. The red line indicates the catch limit of 470029 t established by the HCR for 2018 – 2020. Gear codes are described in Section 2.3.

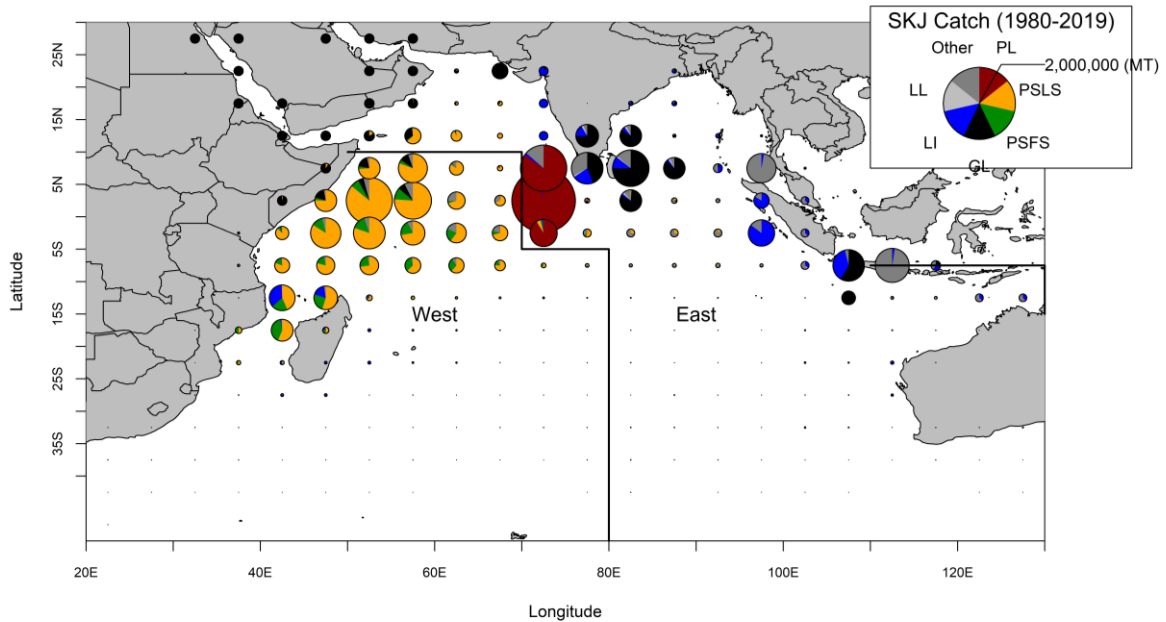


Figure 2: Spatial distribution of Indian Ocean skipjack catches by main fisheries aggregated for 1980-2019. Gear codes are described in Section 2.3. Areas used in two-area spatial structure model (rather than the 80 degree line, Maldives Atoll and Arabian sea are included in the East).

2. OBSERVATIONS AND MODEL INPUTS

Data used in the stock assessment of skipjack tuna using SS3 consist of catch, length frequency data for the fisheries defined in the analysis, relative abundance indices and tag-recapture data. The details of the configuration of the fishery specific data sets are described below.

2.1 Spatial stratification

There remains an open question of the appropriate spatial structure to use for skipjack tuna. Following the approach in previous assessment, two spatial structured options were examined:

IO model

This model examined the entire Indian Ocean as one homogeneous area, with the different fisheries harvesting different portions of the skipjack population. The tagging data suggest that SKJ migrate quickly but the limited distribution of tag releases, and small number of returns outside of the European/Seychelles purse seine fleets (mainly operating in the western equatorial Indian Ocean) makes it difficult to quantify large-scale movements. It is notable that basin-scale movements into the eastern Indian Ocean were observed from the EU/Seychelles fleet, but proper mixing might never occur at the basin scale. Thus, the inclusion of the tagging data in the aggregated spatial structure may induce bias due to the low mixing rates. Another concern is that Maldives PL CPUE is used as an index of abundance for the broader population in the aggregated model when in fact it is derived from the relatively small area of the Maldives EEZ.

IO2 model

The second model assumed that there are discrete populations west and east of 80° (with the exception of the East Indian Ocean including the Maldives and Arabian seas regions, Figure 2). This partition is based on the distribution of major fisheries and appears well fitted with geographical scale of the observed skipjack movements in the western Indian Ocean. The mixing rate is probably quite low between the Northern and southern western Indian Ocean (Iran and Mozambique Channel) because of the large distance between these 2 areas (Fonteneau 2014). Thus, the partition also allows for spatial heterogeneity in tag mixing and changes in abundance. The spatial stratification is a slight modification to the alternative spatial structure examined in the previously assessment which did not appear to provide credible estimates of regional biomass distribution (IOTC-2017-WPTT19).

2.2 Temporal stratification

The population was assumed to be in unfished equilibrium in 1950, the start of the catch data series. The model was iterated from 1950 to 2019, using two alternative temporal time-step:

SS3 internal year-season structure (SSYS)

The population dynamics were represented with an annual/four season configuration, referred as the SS3 internal year-season (SSYS). The model was iterated on quarterly time-steps, to represent potentially important seasonal dynamics, over the period. The tag ages are assigned to annual increments and the spawning biomass is calculated once a year.

Calendar season as model year structure (CSMY).

The alternative option is to define quarterly time periods as years, i.e. each model “year” is a three-month period (and each age class is 3 months). This temporal configuration allows seasonal recruitment to be generated from the stock-recruitment relationship (rather than apportioned among four seasons from a single recruitment event) and allows the tag release to be grouped by finer age classes.

The previous assessment (Fu 2017) provided a detailed analysis of the two temporal configurations but revealed no defect of either option. The CSMY model structure is thought to be suitable for tropical tuna species where growth is fast and spawning is continuously (Langley 2016a, b, McKechnie et al. 2016), but the SSYS model appears to be adequate in modelling most of the population processes at a finer temporal resolution, such as growth, selectivity, and recruitment, in a manner that is either equivalent or closely approximate the CSMY structure (e.g., the SSYS model is able to track the tag dynamics of biologically different cohorts by distributing each tag release age group among seasonal recruitment cohorts). For this assessment, the SSYS model is used for the final model options, and the CSMY model is examined briefly as a sensitivity.

2.3 Definition of fisheries

SS3 requires the definition of fisheries that consist of fishing units with similar selectivity and catchability characteristics. Seven fleets were defined on the basis of gear and fleet of operation:

1. PL – Maldivian Pole and Line fleet.
2. PSLS - FAD/log associated Purse Seine (PS) sets from the EU/Seychelles fleets.
3. PSFS - unassociated PS sets from the EU/Seychelles fleets.
4. Gillnet - includes primarily gillnet fleets from Sri Lanka, Iran, Indonesia and Pakistan
5. Line - includes primarily handline, troll, and small coastal longline gears from Yemen, Sri Lanka, Maldivian, and Madagascar.
6. Longline – a trivial catches from Distant water longline fishing fleets
7. Other – includes all other fleets, primarily non-EU/Seychelles PS fleets, and small coastal fleets (e.g. ring nets).

In the previous assessments, the “*Other*” fleet was defined broadly to have aggregated gillnet, line, longline fisheries (in total four fisheries were defined for the assessment). Consequently, the ‘Other’ fishery included a heterogeneous mix of fleets which caught different sizes of fish (e.g. the longline generally caught much larger skipjack than other gears). The combined size distribution was unlikely to be representative of this composite fleet if the component fisheries had inconsistent size sampling over time. Therefore, it was decided to partition this composite fleet into fisheries with distinctive selectivity characteristics, with the aim to improve predicted sizes in the catch and the estimates of the selectivity patterns.

2.4 Catch history

The total catches were calculated by the Secretariat (IOTC 2020). The nominal catches are not always reported by species and/or gear by the responsible institutions in each country. The catches reported under species and/or gear aggregates are decomposed by the IOTC secretariat using alternative sources of information (if available), or a pre-defined criterion so that all catches are separated into individual gears and species. The catch time series for the 7 fleets is shown in

Figure 1.

Total Skipjack catches in the years 1987-2018 have been relatively impacted by the revisions introduced to the official catch series submitted in late 2019 by Pakistan for its gillnet fisheries, with revised catches being now 69,244 MT lower (in total) during considered years (IOTC 2020).

2.5 CPUE indices

2.5.1 Maldives PL CPUE series

Medley et al. (2020) updated and revised the abundance index for skipjack tuna from Maldives pole and line catch and effort data. The index was derived from multiple datasets with differing level of detail over the period 1970–2018, which represented a considerable revision and improvement to the previous index covering only 2004–2017. The standardisation undertaken using a Bayesian approach has accounted for missing mechanization information on the fleet 1974–1979, and included additional fishing power effects estimated using subjective priors based on an expert meeting (Figure 3).

The main concern on this CPUE is that the spatial area in which the Maldives pole and line operates may not represent the Indian Ocean, and thus the index may be more appropriate as a regional abundance index. The substantial decline in the abundance index during 1970–1980 when the Indian ocean skipjack fishery was not much developed may to some extent reflect local depletion and could result in inconsistent stock dynamics by the assessment model when reconciling this large decline with the relatively small catches. The index also showed a steeper decline than the previous index for the overlapping period (see Figure 3). The WPTT22 Data Preparatory meeting suggested that the time series covering 1995–2018 are probably more reliable and could be considered for the configuration of a base model (IOTC–WPTT22(DP) 2020).

2.5.2 EUROPEAN PSLs abundance indices series

The European and associated flags purse seine fishing activities in the Indian Ocean during 1981–2020 have been monitored through the collection of logbook and observer sampling. A standardized index of the abundance of skipjack caught by the European purse seiners (Spain and France) under floating objects (including primarily sets on drifting fishing aggregating devices) was developed covering 1986–2019 (Guery, et al. 2020, Figure 4). The standardization was based on the application of a generalized linear mixed model which considered a comprehensive list of candidate covariates, including non-conventional covariates.

2.5.3 EUROPEAN PSLs Echo Echosounder Buoys indices

Santiago et al., (2020) developed a novel catch-independent abundance index for skipjack tuna populations based on acoustic data from echosounder buoys: the Buoy-derived Abundance Index (BAI). The BAI assumes of a proportional relationship between the acoustic signal provided by buoys and the tuna abundance, standardized through a modelling approach to account for potential factors other than changes in abundance. The index was used to provide direct estimation of skipjack tuna abundance in the Western Indian Ocean over the period 2011–2019 (Figure 4).

2.5.4 Other abundance indices

Baidai et al. (2020) developed a novel approach to construct estimates of tropical tuna population size based on their associative dynamics with floating objects and acoustic data collected from echosounder buoys. The approach was implemented to provide time series of abundance for skipjack tuna in the western Indian Ocean, over the period 2013 to 2019 (Figure 4).

Guery et al. (2020) also provided a standardized index of skipjack tuna caught by the European purse seiners for unassociated fishing sets (free schools). However, the purse seine catch on free schools has been very small in recent years and therefore the index might not be representative of the stock

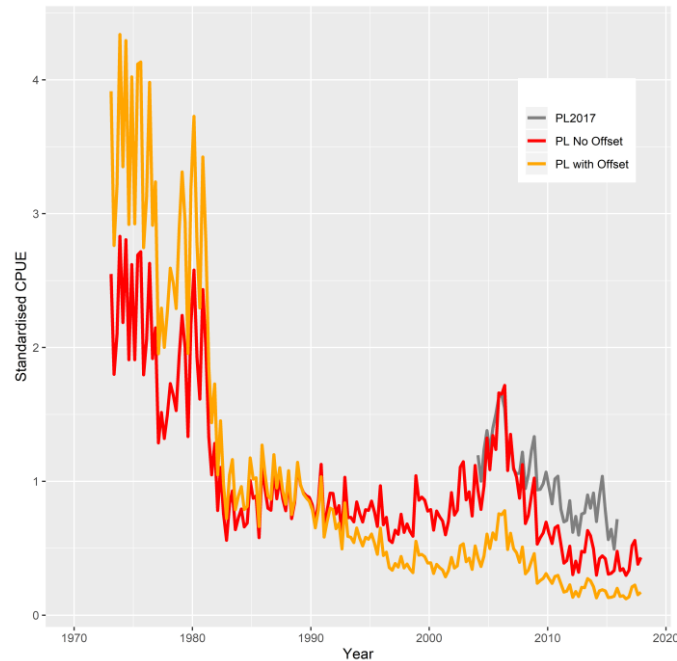


Figure 3: Standardised CPUE derived from the Bayesian GLM model for the Maldives PL fisheries 1970 – 2018: PL No Offset – index that did not include the subjective expert option on changes of fishing power; PL with Offset – index that included the expert option; PL2017 – index covering 2004 – 2017 used in the previous assessment.

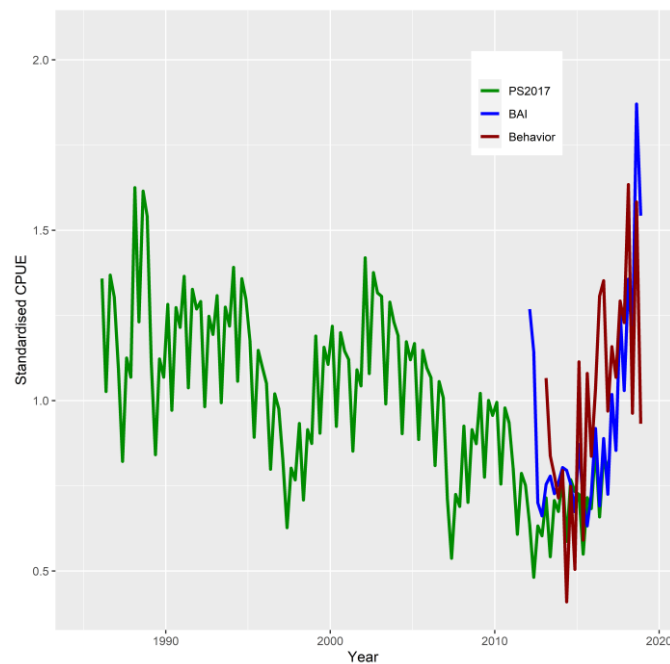


Figure 4: Standardised CPUE for the European PS fleets, derived from (1) catch effort data from associated schools 1986 – 2019, (2) Buoy-derived Abundance Index (BAI) 2012 – 2019, and (3) associative dynamics with floating objects and acoustic data 2013 – 2019 (Behaviour).

2.6 Length frequency data

Available length-frequency data for each of the defined fisheries were compiled into 27 3-cm size classes (20–22 cm to 98–100 cm) and were aggregated to provide a composite length composition for each year/quarter. Each length frequency observation for purse seine fisheries represents the number of fish sampled raised to the sampling units (sets in the fish compartment) while for fisheries other than purse seine each observation consisted of the actual number of skipjack tuna measured. In the assessment, all length composition strata from all fleets were down-weighted by dividing the number of fish included in the aggregated sample by a factor of 1000, with a maximum initial sample size of 10. The *Other* fleet was further down-weighted to have a maximum initial sample size of 1, because it represents a heterogeneous mix of fisheries, many of which are poorly sampled.

Aggregated Catch-at-length distributions for each fishery are shown in Figure 5. The bimodal distribution in the PL fishery suggests a heterogeneous mix of two life history stages. Brief exploration did not reveal any obvious spatial/seasonal explanation for the two modes. Size data for Maldivian PL from 1987 to 2000 have been removed from the database as they are considered extremely unreliable. Similarly, the data for 2015/2016 was removed as only extremely small fish (less than 1kg on average) were reported.

The recent decline in mean size in the *Other* fleet probably reflects the erratic sampling from this fleet. It has been noted previously that the length frequency data from Thailand small purse seiners in 2007 and following years were of extremely poor quality. For the ‘Other’ category, size data between 2007 and 2010 were not used.

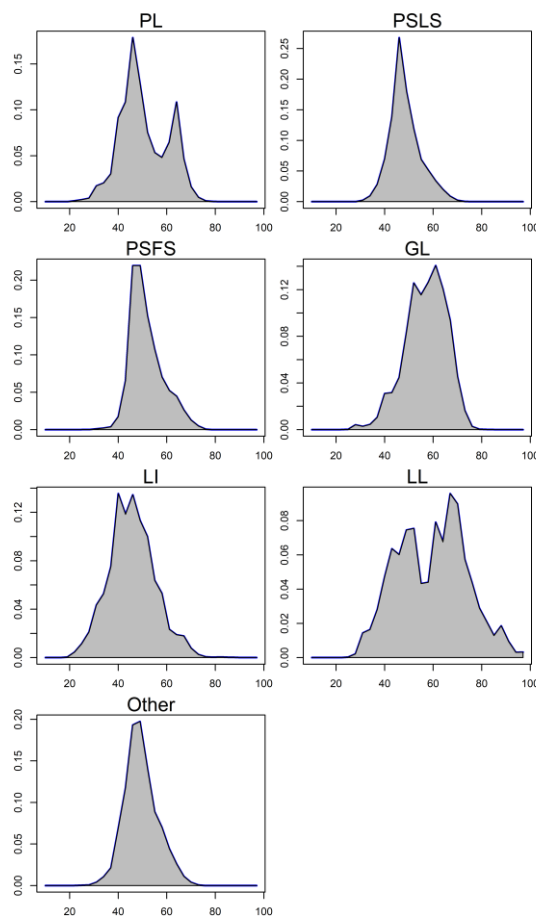


Figure 5: Length compositions of skipjack tuna samples aggregated by fishery.

2.7 Tagging data

A considerable amount of tagging data was available for inclusion in the assessment model (Hallier & Million 2009). Between 2005 and 2007, about 77000 tagged skipjack were released from Tanzania, Seychelles and Mozambique Channel under the RTTP-IO program (Figure 6). Additional tagging (~22000 releases) also occurred in the eastern Indian Ocean as part of small-scale tagging operations in 2004–2009 (Figure 6). The most substantial small-scale project was based in the Maldives (Jauharee & Adam 2009), but tags were also released near Lakshadweep, Mayotte, western Sumatra and the Andaman Islands.

Most skipjack tagged under the RTTP-IO were under 2-year of age (Figure 7). The percent of returns for the RTTP-IO tags is approximately 16% and the returns were primarily from the purse seine fishery in the western Indian Ocean within four years after release (Figure 8,

Table 1). A significant proportion of the tag returns from purse seiners were not accompanied by information concerning the set type. These tag recoveries were assigned to either the free-school or FAD fishery based on the proportion of catch by each fishing mode. The low number of returns from other fisheries is partly due to lower catch numbers, particularly of the smaller size classes that were tagged, but probably due in most part to non-reporting (Eveson 2012 et al.).

In contrast smaller fish was tagged under the small-scale program (Figure 7) and the percent of tag returns is approximately 12% (

Table 1). The returns were primarily from the Maldives Pole and line fishery (Figure 8), but the numbers were variable over time. In general release cohorts with higher recovery rates were mostly tagged in Maldives waters 2007 – 2009, whereas releases made further east in the IO waters between 2004 and 2006 tend to have lower recovery rates. The recovery from the purse seine fishery is extremely low (less than 10 recoveries except for those released in the first two quarters of 2009).

The RTTP-IO data is considered more reliable than the small-scale tagging programs, because the RTTP-IO has a much larger number of tags and was released by more experienced taggers. In contrast, there was no tag shedding estimates for the fleets conducting the small-scale tagging programs, and the reporting rates from pole and line fishery were also unknown. The previous assessment included the small-scale data in part of the model grid considering that the small-scale tagging program may provide additional insight into spatial dynamics. However, the inclusion of the small-scale data is likely to introduce bias to the model estimates because (1) the recovery rate of small scale tags from the PS fishery is extremely low (the tag returns from the PS fishery is the primary source of information on abundance), and (2) very few tags (<5%) were recovered with a time of liberty exceeding 2 quarters, whereas it is generally agreed that longer periods are required to achieve sufficient tag mixing. For this assessment, the small-scale tag data is only included in a sensitivity model.

For incorporation into the assessment model, tag releases were stratified by release region, time period of release (quarter) and age class. The returns from each tag release group were classified by recapture fishery and recapture time period (quarter). The tag data were further adjusted for tag losses and reporting rates to minimize the bias on estimates of fishing mortality and abundance in the assessment model. The procedure is described in below.

Age assignment of tag release. The length of release of each tag is recorded in the database but the model dynamics are based on ages. The age of each individual tag was estimated from the mean of the growth curve, assuming a 1 January birthdate. The age estimation occurs external to the model.

Tagging mortality. The number of tags in each release group was reduced by 25% to account for initial tag mortality. Tagging mortality was estimated relative to those for the best tagger (Hoyle *et al* 2015). Hoyle et al. (2015) did not find any differences in tagging induced mortality between species in the Indian Ocean but tag mortality was estimated to be lower for skipjack in the Pacific Ocean where there are more data.

Reporting rate. The results of the tag seeding experiments conducted during 2005–2008, have revealed considerable temporal variability in tag reporting rates from the IO purse-seine fishery (Hillary *et al.* 2008a). Reporting rates were lower in 2005 (57%) compared to 2006 and 2007 (89% and 94%). Quarterly estimates were also available and were similar in magnitude (Hillary *et al.* 2008b). This large increase over time was the result of the development of publicity campaign and tag recovery scheme raising the awareness of the stakeholders, *i.e.* stevedores and crew. SS3 assumes a constant fishery-specific reporting rate. To account for the temporal change in reporting rate, the number of tag returns from the purse-seine fishery in each stratum (tag group, year/quarter, and length class) were corrected using the respective estimates of the reporting rates. Following Kolody (2011) and Fu (2017), tags recovered at-sea are assumed to have a 100% reporting rate; tags recovered from landings in Seychelles were corrected for the quarterly estimates of reporting rates from Hillary *et al.* (2008b). The tag recoveries were further increased by the proportions of EU PS catches landed outside the Seychelles, to account for purse-seine catches that were not examined for tags. For example, the adjusted number of observed recaptures for a PSLS fishery as input to the model, R'_L was calculated using the following equation:

$$R'_L = R_L^{sea} + \frac{R_L^{sez}}{p^{sez}r^{sez}}$$

where

R_L^{sea} = the number of observed recaptures recovered at sea for the PSLS fishery.

R_L^{sez} = the number of observed recaptures recovered in Seychelles for the PSLS fishery.

r^{sez} = the reporting rates for PS tags removed from the Seychelles

p^{sez} = the scaling factor to account for the EU PS recaptures not landed in the Seychelles.

The adjusted number of observed recaptures for a PSFS fishery was calculated similarly. A reporting rate of 94% was assumed for the correction of the 2009–2015 tag recoveries. The numbers of tag recoveries were also adjusted for long-term tag loss (tag shedding) based on an analysis by Gaertner and Hallier (2015). Tag shedding rates for skipjack tuna were estimated to be approximately 3% per annum.

For the RTTP-IO, a total of 58 420 releases were classified into 40 tag release groups. Most of the tag releases were under age 2 (Figure 7) A total of 10458 actual tag recoveries were included in the tagging data set. The cumulative effect of processing the tag recovery data increased the number of recoveries to 11,640 tags.

Table 1: Number of Tag releases by year (of release) and recoveries by year (of recovery) for the skipjack tuna RTTO-IO and small scale tag Programs.

RTTP Release		Recovery							
		2004	2005	2006	2007	2008	2009	2010	2011
2005	14744		160	1592	277	26	2		
2006	41387			2793	4277	303	39	5	
2007	21741				1901	1019	167	9	
SS Release		2004	2005	2006	2007	2008	2009	2010	2011
2004	4339	254	39	6	3	2			
2005	2208		51	35	3				1
2006	2883			176	19	2			3
2007	741				29	19	8	3	
2008	5029					383	180	2	
2009	7233						1440	39	2

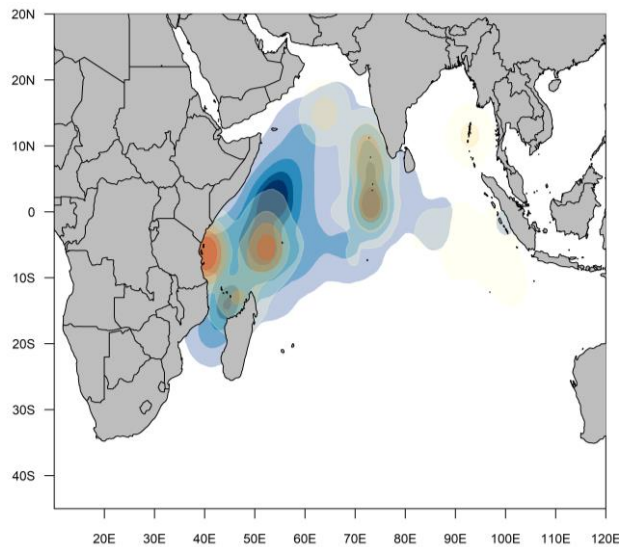


Figure 6: Location of releases (red) and density of recoveries for the skipjack tuna RTTO-IO and small-scale tag Programs

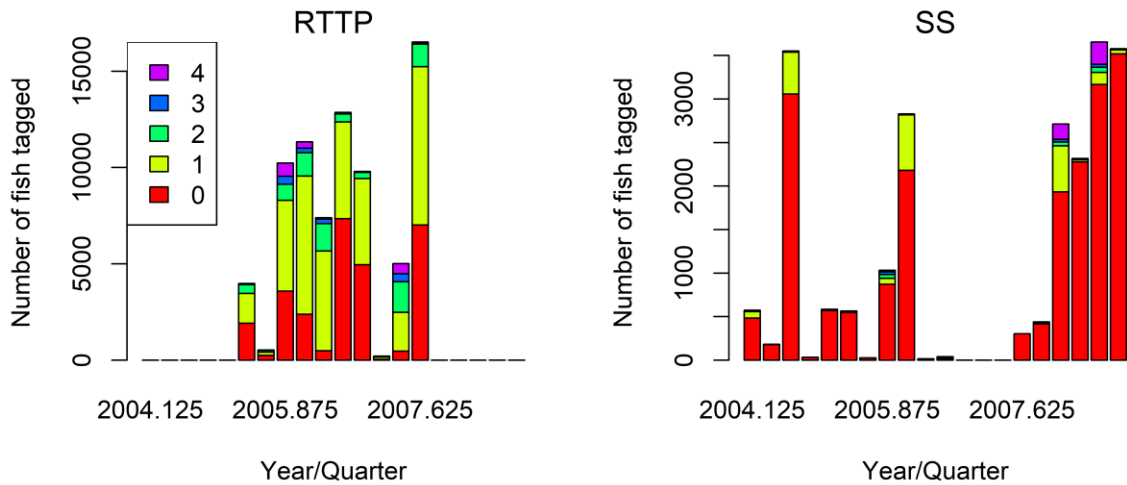


Figure 7 : Number of tag releases quarter and age class for the skipjack tuna from the RTTO-IO and small-scale tag Programs. Ages were assigned based on the length.

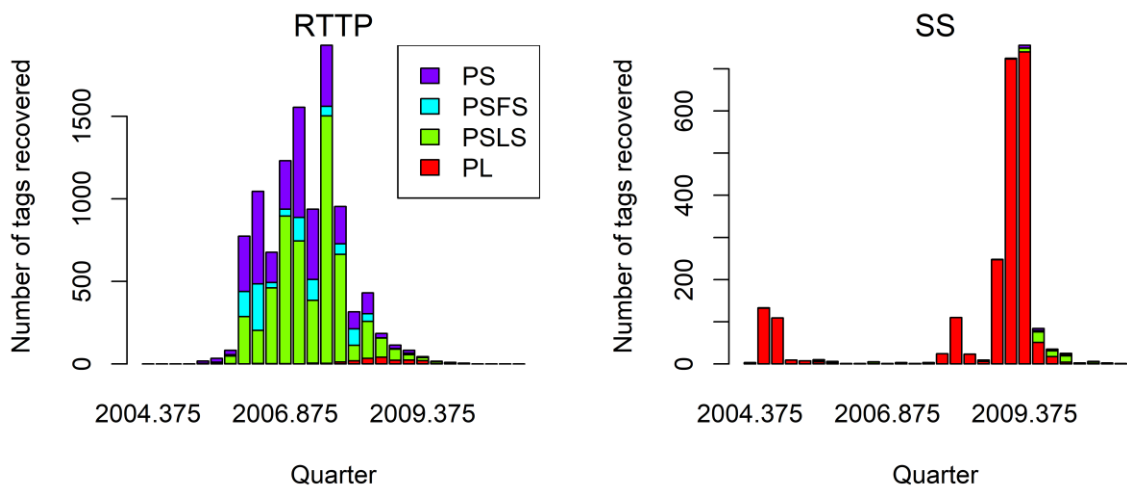


Figure 8: Number of tag recoveries by year/quarter and fishery for the skipjack tuna from the RTTO-IO and small-scale tag Programs. Purse seine tag recoveries have not been corrected for reporting rate.

3. MODEL STRUCTURAL AND ASSUMPTIONS

3.1 Population dynamics

The dynamics described below pertains to the aggregated spatial model with the year-season structure (the IO model).

The model was sex-aggregated (and reported spawning biomass is the summed mass of all mature fish). The stock assessment model partitioned the Indian Ocean skipjack age groups 0–8 years with the last age a plus group (in unfished equilibrium, <0.25% of the population survives to reach the plus-group with the constant M value considered).

The population was assumed to be in unexploited equilibrium in 1950, the start of the catch data series. The model was iterated from 1950-2019 using a quarterly time-step. The nominal unit of time in the model is one year during which population processes (e.g., recruitment, spawning, and ageing) were applied in sequence according to the dynamics implemented within the Stock Synthesis model (Methot 2013). The Observations were fitted to model predictions on the seasonal basis within the year.

An alternative model option commenced in 1970 and assumed an exploited, equilibrium initial state, considering that the main fisheries were developed after 1970 and there is almost no data prior to that. Initial fishing mortality parameters were estimated for each of these fisheries, based on early catches. The resulting fishing mortality rates are applied to determine the initial numbers-at-age. This model option yielded very similar results and thus was not reported further.

3.1.1 Recruitment

For some of the tuna species there is an indication of a strong seasonal pattern in recruitment (Adam Langley per. comm.). However, Itano (2000) suggested tropical tuna spawning does not always follow a clear seasonal pattern but occurs sporadically when food supplies are plentiful. SKJ has been assumed to have a continuous spawning season.

Recruitment was assumed to occur annually at the start of the year and the SS3 will allocate recruitment to each season (the population will have a collection of seasonal cohorts with different birthdays), with the proportion being estimated as time-varying parameters. New recruits enter the population as age-class 0 fish (averaging approximately 20 cm). A Beverton-Holt stock recruitment relationship was assumed with steepness fixed at a range of options. ISSF (2011) summarises steepness estimates from tuna fisheries, the high values reported seem to be consistent with SKJ life history. The final model options included three (fixed) values of steepness of the BH SRR (h 0.7, 0.8 and 0.9). These values are considered to encompass the plausible range of steepness values for tuna species such as bigeye tuna and are routinely adopted in tuna assessments conducted by other tuna RFMOs.

Annual deviations from the stock-recruitment relationship were estimated for 1983–2018, assuming a lognormal distribution. Assessments of major tropical tuna species using a quarterly model time-step typically assumed the quarterly recruitment events to have a fixed standard deviation (σ_R) of 0.6 for recruitment deviates (Kolody et al. 2018), corresponding to an annual CV of about 0.3 (assuming quarterly recruits are independent and the annual recruitment is calculated as the mean of four seasonal events).

3.1.2 Growth and Maturation

Skipjack growth is rapid compared to yellowfin and bigeye tuna. Young skipjack is approximately between 10–20cm as age of 40–90 days after hatching and immature fish is approximately in a range of 20 cm to 40 cm as age of 90 days to one year after hatching (Kiyofuji, 2019). Earlier assessments have considered length-at-age relationships that followed the standard von Bertalanffy growth function. But there were concerns that the von-B growth curves might not be capturing the rapid initial growth rate for this species (e.g. Kayama et al. 2009). The 2017 assessment adopted a two stanza VB-logK curve of Eveson (2012), derived from the tag-recapture data. The VB-logK curve was approximated using a Richards curve in SS3, with $L_{inf} = 70\text{cm}$, $k=0.34$, and the inflexion parameter fixed at 2.96. However, the L_{inf} appears to be low compared to the Pacific, where a number of estimates suggested maximum length above 80 cm. The two-stanza growth is considered to be appropriate for skipjack tuna as it captures the rapid growth of juveniles, and diminished growth from a transfer of energy from somatic growth to gonad development (Grande et al. 2010). A CV of 0.2 and 0.1 is assumed for the length at the initial and maximum age, respectively with linear interpolations for intermediate ages (Figure 9–left), loosely based on evidence from tagging data.

Maturity was estimated by Grande *et al.* (2010): invariant over time with 50% maturity at length 38 cm (Figure 9–right), corresponding to an age-at-maturity of 0.4 y with the Richard growth curve. This is also very similar to the 40 cm value reported in the Pacific, where the maturity is estimated to follow a knife-edge pattern with all fish two quarters or less being immature and all fish older being fully mature (Vincent *et al.* 2019). The weight-length relationship was estimated from Chassot *et al.* (2016), where $W = 4.97e-006 L^{.39292}$.

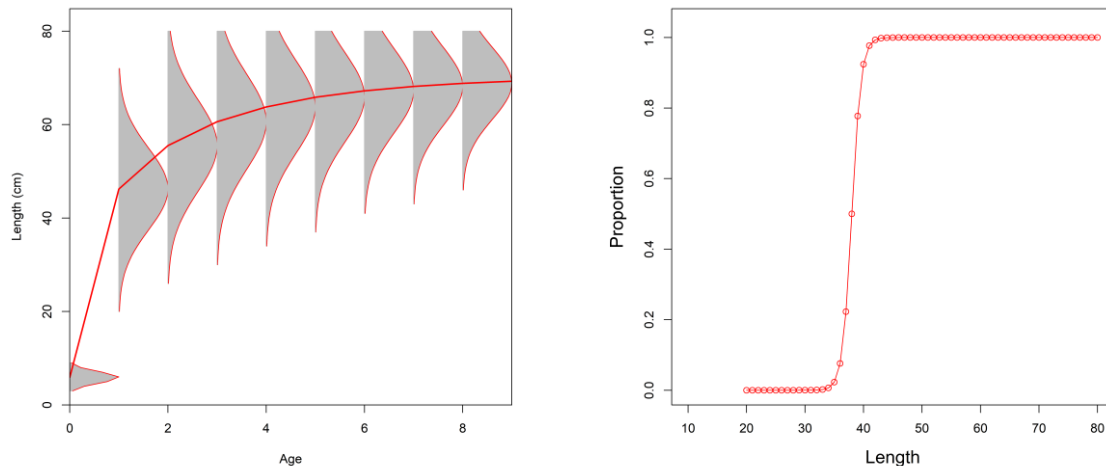


Figure 9: Fixed growth function for skipjack tuna following Eveson *et al.* 2012 (left) and length-based maturity Ogive following Grande *et al.* (2010). For the growth function, the red line represents the estimated mean length (FL, cm) at age and the grey area represents the assumed distribution of length at age).

3.1.3 Natural mortality

Independent estimates of natural mortality for skipjack tuna were available from tagging data (Eveson 2011) but the estimates appeared to be very low compared to the assumed or estimated M in the other oceans. For the assessment, the natural mortality of 0.8 (constant across all ages) is used, which is the equal to the value used by the ICCAT). Previous assessment also considered estimating M within the model when the small-scale tagging data were included, and the estimates were similar in magnitude to the assumed value of 0.8.

3.2 Fishery dynamics

Length based selectivity were assumed for all fisheries. Within the model, the length-based concept is used to calculate the predicted catch-at-length distribution. Selectivity is converted to an age-based selectivity for purposes of removing the appropriate portion of the population in the catch. A non-parametric, cubic spline function was estimated independently for the selectivity of pole and line, and purse seine fleets (both PSLS and PSFS). The function is flexible enough to represent polymodal functions (and was motivated by the clear bimodal distribution of the PL fleet). Seven nodes were estimated for the PL fleet, and 5 nodes for the PSLS, PSFS fleets. The selectivities of the Gillnet and Line fisheries were estimated using a dome-shaped, double normal functional form, and the selectivity of the longline fisheries was estimated using a monotonically increasing, logistic function.

Fishing mortality was modelled using the hybrid method that estimates the harvest rate using Pope's approximation and then converts it to an approximation of the corresponding F (Methot & Wetzel 2013).

3.3 Dynamics of tagged fish

In the population model, tagged fish are assumed to have identical dynamics to the general population. Therefore, a reasonable period of mixing is required before this assumption would be valid. Tag displacement appears to suggest rapid mixing within the core PS area. However, this would be contingent upon the distribution of fishing effort (i.e. if the gear is deployed a long way from the release site, all recoveries will suggest rapid movement, but they might not represent the movement of the general population). Also, directed seasonal migration can cause large displacements, without necessarily resulting in uniform mixing. Final model options included assumptions on mixing periods of 3 and/or 4 quarters. However, for the sensitivity model that included small scale tag data a mixing period of 2 quarter was assumed as there are so few tag recoveries with a time of liberty exceeding 2 quarters.

3.4 Modelling methods, parameters, and likelihood

The total likelihood is composed of four main components: catch data, the abundance indices (CPUE), length frequency data and tag release/recovery data. There are also contributions to the total likelihood from the recruitment deviates and priors on the individual model parameters. The model was configured to fit the catch almost exactly so the catch component of the likelihood is very small. There are two components of the tag likelihood: the multinomial likelihood for the distribution of tag recoveries by fleets over time and the negative binomial distribution of expected total recaptures across the model region.

Assumed CV of 10% (lognormal observation errors) was applied to both standardised CPUE indices. The CV of 10% is not realistic for these fisheries, but it allows the model to fit the core features of the relative abundance series. Higher CV values (e.g. 20%) were examined in a sensitivity model.

For all fisheries, except for the other fisheries, the individual length frequency observations were assigned a maximum effective sample size (ESS) of 10. For the other fisheries an ESS of 1 was assigned to all length observations. The influence of size composition data on the assessment model was examined through several diagnostic tools.

The negative binomial distribution allows for overdispersion relative to the ideal, independent movement, fully mixed, tag recovery distribution (e.g. which might be expected to conform to the Poisson distribution). The overdispersion parameter τ was fixed at 20 and was applied equally across all tag groups. Previous assessments attempted to estimate τ but the estimate was strongly driven by prior.

The parameters estimated by the model included:

- Catchability for the CPUE series
- Selectivity parameters
- Virgin recruitment
- Annual recruitment deviations from the stock recruitment relationship
- Annual seasonal-specific recruitment deviations

The Hessian matrix computed at the mode of the posterior distribution was used to obtain estimates of the covariance matrix, which was used in combination with the Delta method to compute approximate confidence intervals for parameters of interest.

3.5 Reference points

The IOTC Resolution 15/10 has defined interim reference points for the skipjack tuna based on MSY. However, the Skipjack tuna HCR adopted by IOTC (Res.16/02) has an output of a total annual catch limit based on a relationship between stock status (spawning biomass relative to unfished levels) and fishing intensity (exploitation rate relative to target exploitation rate). Therefore, the assessment reports depletion-based reference points in accordance with the key HCR control parameters, including $SSB_{40\%}$, which is 40% of unfished spawning biomass, $F_{40\%SSB}$, which is exploitation rate corresponding to an equilibrium spawning biomass of 40% unfished level, and $Yield_{F_{40\%SSB}}$, which is the corresponding equilibrium catch if fishing at $F_{40\%SSB}$.

4. ASSESSMENT MODEL RUNS

The approach we have taken here is to explore a range of model assumptions and parameter configurations, and to examine areas of uncertainty that would impact assessment results. A basic model was identified, and a range of diagnostic analyses were conducted. Final model options included a grid of models running over permutations of plausible parameters and/or model settings, from which the uncertainty was quantified. The grid approach aims to provide an approximate understanding of variability in model estimates due to assumptions in model structure, which is usually much larger than the statistical uncertainty conditional on any individual model (McKechnie et al. 2016, Kolody et al. 2011). The assessment was conducted using the 3.30 version of the Stock Synthesis software. The stock status was reported for the terminal year of the model (i.e. 2019).

4.1 2017 model continuity run

In the 2017 assessment, no explicit base case model was chosen, and the final model options selected for management advice included 48 models with alternative assumptions on levels of steepness, tagging program options, tag mixing period, tag release mortality, and natural mortality (IOTC–WPTT19). The model *io_h80_MAt_t3_rttp_tm25m* (steepness of 0.8, constant M, RTTP tag program, tag mixing period of 3 quarters, and tag release mortality of 25%) was considered as a reference model (Fu 2017). The 2017 reference model was updated sequentially to ensure a level of continuity, and to assess the influence of the additional data available. The model period was extended to 2019 with incremental changes made to the observational data and other configurations (see Table 2 for details).

Table 2: Description of the sequence of model runs to update the 2017 reference model

<i>Model</i>	Description
<i>io_h80_MAt_t3_rttp_tm25m</i>	2017 reference model
<i>Update-1Fleet</i>	The composite ‘Other’ fishery further separated into Gillnet, Line, Longline, and a miscellaneous ‘Other’ fishery group.
<i>Update-2Catch</i>	Model extended to include 2016–2018, with updated catches
<i>Update-3Data</i>	Revised and updated length composition data, PL CPUE index 2004 – 2018, PSLs index 1990 – 2019

4.2 Basic and sensitivity models

On basis of the model updates, minor revisions were made to attain a basic model (Table 3), which served as a starting point for the sensitivity analysis and development of the final model grid. The basic and sensitivity models examined a range of model options related to the CPUE series and tagging data, biological parameters and model structure. The analysis complemented the suite of exploratory models conducted previously, with the aim of determining a suitable ensemble of model options to capture a range of uncertainty on stock estimates. Table 4 provides a description of the alternative model options considered for the sensitivity analysis.

Table 3: Main structural assumptions of the basic model and details of estimated parameters. Changes to the 2017 assessment are highlighted in red.

Category	Assumptions	Parameters
Recruitment	Occurs at the start of each quarter as 0 age fish. Recruitment is a function of Beverton-Holt stock-recruitment relationship (SRR). Seasonal apportionment of recruitment with temporal deviates 1983 – 2015 Temporal recruitment deviates from SRR, 1983–2018.	R_0 Norm(10,10); $h = 0.80$ $PropR2$ Norm(0,1.0) $SigmaR = 0.6$.
Initial population	A function of the equilibrium recruitment in each region assuming population in an initial, unexploited state in 1950.	
Age and growth	8 age-classes, with the last representing a plus group. Growth based on a Richard growth model which approximate the two-stanza growth estimated by Eveson <i>et al</i> (2012). SD of length-at-age based on a coefficient of variation decreasing linearly from 20% at age 0 to 10% at maximum age. Mean weights (W_j) from the weight-length relationship $W = aL^b$.	$L_{infinity} = 70$ cm, $k = 0.35$, Richard parameter of 2.90.
		$a = 4.97 \text{ e-}06$, $b = 3.39$
Natural mortality	Constant at 0.8	
Maturity	Length specific logistic function from Grande et al. (2010). Mature population includes both male and female fish (single sex model).	Mat50_Fem 38 cm Mat_slope_Fem -1.25
Selectivity	Cubic spline (7 nodes) selectivity for PL Fishery Cubic spline (5 nodes) selectivity for PSLS and PSFS Fisheries Double normal selectivity for Gillnet, Line, and 'Other' fisheries Logistic selectivity for the longline fishery	Logistic $p1$ Norm(40,40), $p2$ Norm(10,10) Double Normal Five or seven node cubic spline
CPUE indices	PL index 1995 – 2018; PSLS index 1990 – 2019. Temporally invariant catchability	Unconstrained parameter PLq , and $PSLSq$
Fishing mortality	Hybrid approach (method 3, see Methot & Wetzel 2013).	
Tagging data	Included only tag release from the RTTP program, and EU PS tag recoveries (adjusted for externally estimated reporting rates); tags assumed to be randomly mixed at the model region three quarters following three quarters of release;	PS RR 1.0
Length composition	Multinomial error structure. Length samples assigned maximum ESS of 10.	

Table 4: Description of the sensitivity models for the 2020 assessment. Description of changes are relative to the basic model.

<i>Model</i>	Description
CPUE indices	
<i>PL</i>	Only PL 1995 – 2018 index is included
<i>PSLS</i>	Only PSLs index is included;
<i>PL1975</i>	Extend PL index back to 1975.
<i>PLoffset</i>	Alternative standardized PL index 1995 – 2018 which accounted additional fishing power changes (see Medley et al. 2020)
<i>BAI</i>	Included Purse seine buoy-derived abundance index (Santiago et al. 2020), and the index based on the associative dynamics with floating objects and acoustic data (Baidai et al. 2020).
<i>Cv20</i>	A CV of 0.2 for all CPUE indices
Tagging data	
<i>rtss</i>	Included both RTTP and small-scale tag releases, and PS and PL recoveries; estimated the PL reporting rate.
<i>TagLambda01</i>	Tag lambda = 0.1 for both components of tag likelihood.
<i>TagLambda001</i>	Tag lambda = 0.01 for both components of tag likelihood.
Biological parameters	
<i>growthCV</i>	A larger SD of length-at-age based on a constant coefficient of variation of 0.2
<i>MHighJ</i>	Higher natural mortality values at younger ages (M = 1.5, 1.2, and 1.0 for age 0, 1, and 2)
<i>MHighA</i>	Higher natural mortality values (M=1.2) for ages 2 – 8
Spatial structure	
<i>io2</i>	Eastern and western Indian Ocean two area model; PSLs and PSFS fisheries are assigned to the western region; PL, GI, LI, LL and Other fisheries are assigned to the eastern region; tag releases assigned to the western region
<i>io2TagLambda01</i>	Eastern and western Indian Ocean two area model; tag lambda = 0.1 for both components of tag likelihood.
Temporal structure	
<i>Q4</i>	Calendar seasons as model years (CSMY), as opposed to the SS3 internal year-season structure (SSYS).

4.3 Final model assessable (grid)

On basis of the exploratory analysis, final options were configured to capture the uncertainty related to model structure, assumptions on the stock-recruitment steepness, tag mixing, and tag data weighting, which are thought to contribute to the main sources of uncertainty (Table 5). Thus, the final models involved running a full combination of options on spatial structure (2 options), steepness (3 values), tag mixing period (2 values), and tag lambda (2 values). The final model grid differs to the options adopted for the 2017 assessment: it did not include the option of incorporating the small scale tag data, and it dropped the alternative, lower value of tag release mortality as the WPTT21 agreed that the estimates of Hoyle et al. 2020 should be used. Instead, the new model grid has the addition of an alternative spatial structure and alternative tag data weighting.

Table 5: Description of the final model options for the 2020 assessment. The final models consist of a full combination of options below, with a total of 24 models. The options adopted for the basic model is highlighted.

Model options	Description
<i>Spatial structure</i>	<ul style="list-style-type: none"> • io – whole Indian Ocean one area model • io2 – East and western Indian Ocean two area model;
<i>Steepness</i>	<ul style="list-style-type: none"> • h70 – Stock-recruitment steepness parameter 0.7 • h80 – Stock-recruitment steepness parameter 0.8 • h90 – Stock-recruitment steepness parameter 0.9
<i>Tag weighting</i>	<ul style="list-style-type: none"> • <i>TagLamda01</i> – Tag lambda = 0.1 for both components of tag likelihood. • <i>TagLamda1</i> – Tag lambda = 1 for both components of tag likelihood.
<i>Tag mixing</i>	<ul style="list-style-type: none"> • <i>t3 – Tag mixing period of 3 quarters</i> • <i>t4 – Tag mixing period of 4 quarters</i>

5. MODEL RESULTS

5.1 2017 model continuity run

The 2017 assessment model defined a composite fleet which aggregated several fisheries with distinctive size composition due to concerns of inadequate sampling. Consequently, the size composition of this fleet was influenced by fisheries which contributed very little catches yet had a conflicting trend to other main fleets (e.g. PL and PSLS). This led to some instability of the model, i.e., model estimates appeared to be particularly sensitive to even minor changes of the weighting on the size data. The revision of the fleet structure allows the model (*Update-IFleet*) to better characterise the selectivity pattern for a few important fishery components (e.g. gillnet and line fisheries), alleviating (but not eliminating) the data conflict. The model with the revised fleet structure increased the stock estimates by about 15% on average (Figure 10).

Subsequent model update with only the catch data (*Update-ICatch*) yielded almost identical estimates of historical stock biomass (Figure 10), despite of the revisions made to the historical catches (see Section 2.3). Further updates with observational data (*Update-IData*) has reduced the stock estimates in the late 1980/early 1990s (Figure 10), as a result of the changes in the CPUE series (i.e. the new PSLS CPUE dropped data before 1990, and the new PL CPUE had a steeper decline). Overall, these accumulative changes appeared to have yielded a stock estimate that is broadly similar to the 2017 assessment model (Figure 10).

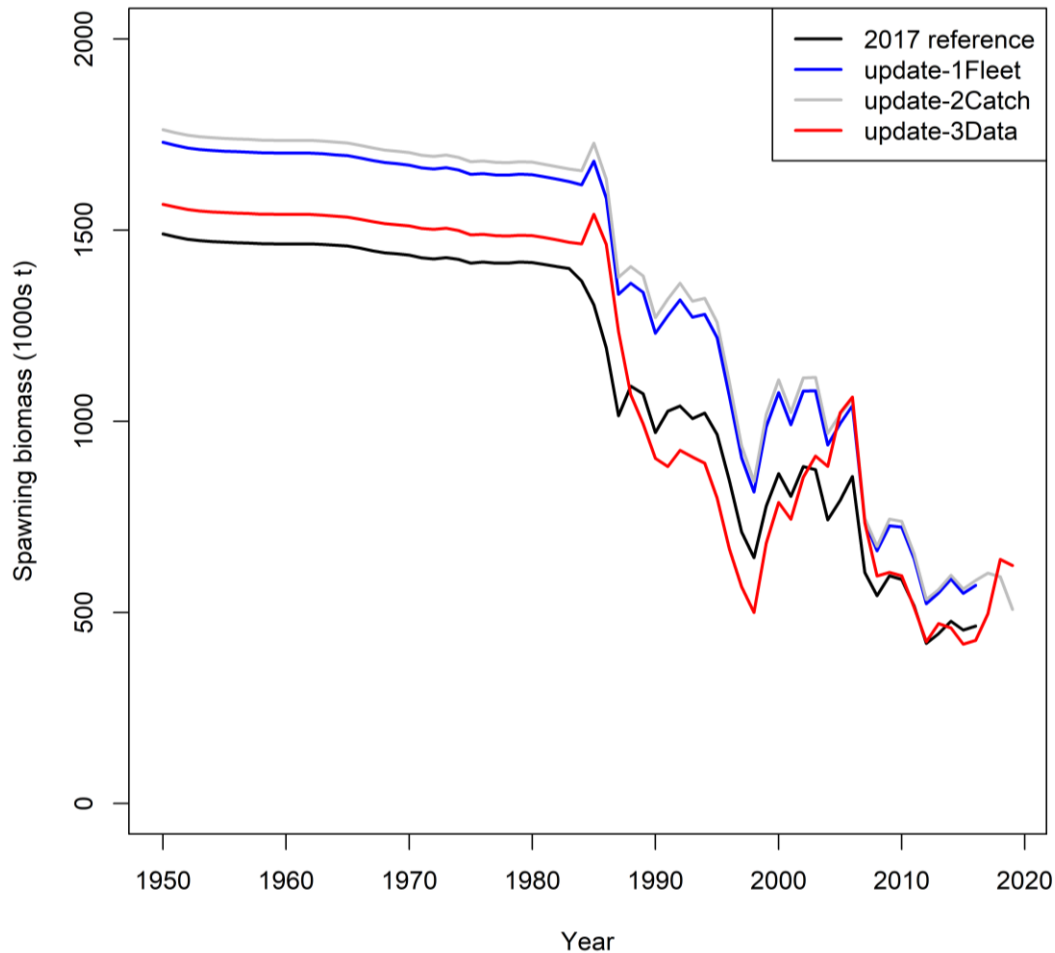


Figure 10: Spawning biomass trajectories for IO skipjack tuna from the stepwise model updates for 2020. (from the 2017 assessment reference model ‘*io_h80_MAt_t3_rtp_tm25m*’).

5.2 Basic models

On basis of the 2017 model updates, a basic model was configured (see Table 3). The basic model extended the PL index back to 1995, based on the recommendation from the WPTT22 Data Preparatory meeting (IOTC–WPTT22(DP) 2020). The other minor revisions included extending the period for the estimation of recruitment deviates to 2017, and the definition of F-age (2018) for the determination of associated reference points (e.g. $F_{40\%SSB}$).

5.2.1 Model fits

The basic model included both the Maldives PL index and EU PS index (as in the previous assessment) with effectively equal weight, assuming that they are indexing the vulnerable biomass of skipjack tuna in the Indian Ocean. This is based on the following considerations: (1) the two sets of index are broadly consistent with each other, in view of their overall increasing trend from 1995 to 2005, and the subsequent decline; (2) both indices corresponds to regional fisheries with limited spatial coverage, and thus complement each other in providing abundance signals for the larger, ocean-wide stock. The model fitted the PL and PS indices reasonably and has adequately captured the inter-annual variability of both time series (Figure 11). However, the difference in the timing of the peak in the two CPUE series caused some misfits in some years, and there are also contrasting trends in the residuals from the fits (Figure 12), which reflected some of the conflicts between the two CPUE series (in terms of the extent of the decline). This may not be a concern given that compromise is expected when fitting multiple abundance indices in a spatially aggregated model. There appears to be no coherent seasonal trend in either time series and the pattern in the predicted indices is due to one or two dominant seasonal cohorts estimated by the model.

The fits to the time series of length frequencies for each of the 7 fisheries are provided in Appendix A (Figures A1). The fits are very reasonable for the main fisheries (i.e. PL, PSLS, and PSFS) where the samples are generally considered to be adequate and representative. For other fisheries, although there is no gross misfit to these data, the fits were poor in some instances (e.g., LI fishery 1986, 2016, 2017; GI fishery 1996, 1997, etc.). For the LL fishery, there are considerable variabilities among individual samples, apparently due to poor sampling (Figures A1). The fits to the fleet-aggregated length frequency appear mostly adequate (Figure 13), indicating that the model has captured the gross features of the length composition data well (thus there is probably no significant bias in the estimates of fishery selectivities). However, there is a lack of fits to the larger fish in the length samples from the longline fishery (see further discussion in Section 5.3), although it is evident that smaller fish were most likely under-sampled. The model appeared to have tracked the mean length in the catches reasonably well – the moderate declining trend in the mean length for all fisheries predicted by the model are generally consistent with the observations, except for the LI fishery (Figure 14), but the large inter-annual variability in the PSFS fishery is not captured well by the model.

The fit to the observed number of tag recoveries was examined for the fisheries which accounted for most of the tag returns (i.e. PSLS). The fit to the number of tag recoveries was examined by recombining the tags into individual release periods (i.e. aggregating the releases by age class) and excluding those recoveries that occurred during the mixing period (Figure 15). The number of tag recoveries varied considerably amongst the release periods and most releases occurred in 2006. Most of the observed tag recoveries in the post mix period were from the PSLS fishery and a high proportion of the total recoveries occurred during the first four quarters following the mixing period (Figure 15). Nonetheless, overall the model under-estimated the number of tag recoveries in the four-quarter period (Figure 15). This may be indicating inadequate mixing of the tags with the fish population vulnerable to the PSLS fishery. Longer-term recoveries were less vulnerable to the PSLS fishery and, hence, numbers of recoveries declined considerably.

The fit to the tag recoveries was also examined by time period (quarters), by age at recovery, and by time at liberty (quarters) for the aggregated data set with all releases combined (Figure 16). Overall, there was a reasonable fit to the tag recoveries from the PSLS fishery during the main tag recovery period (to 2010) but the model over-estimates the number of longer term tag recoveries from the older age classes (at recovery), i.e. those fish at liberty for a longer period (Figure 16), this may reflected variable tag reporting over time or mis-specification of natural mortality. However, the model provides a reasonable prediction of the longer-term tag recoveries from the PSFS fishery (Figure 17).

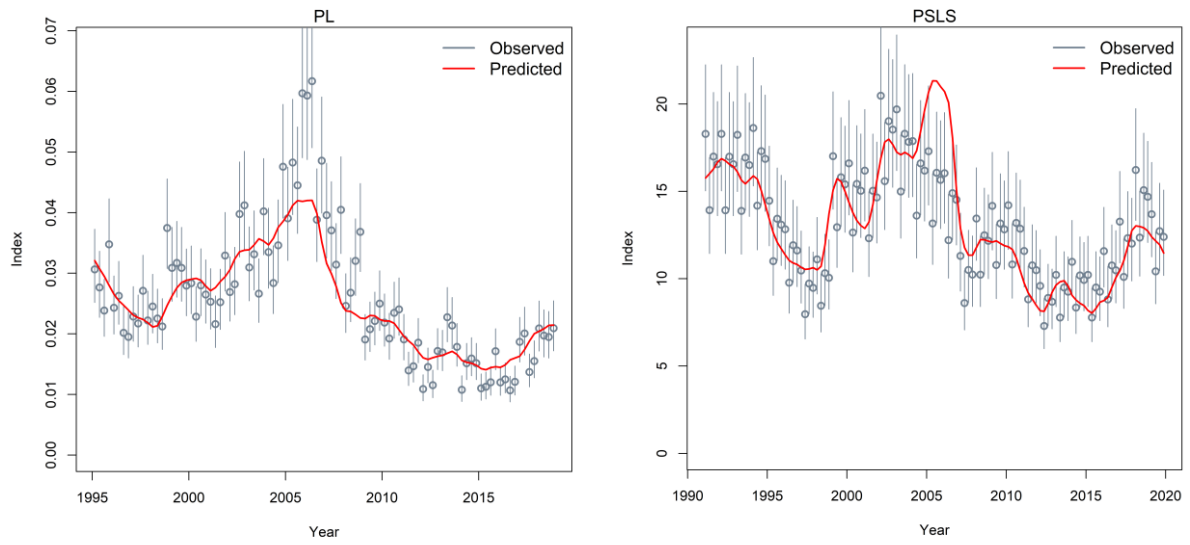


Figure 11: Fits to Maldives PL CPUE 1995 – 2018 and the EU PS CPUE 1991 – 2019 for the basic model.

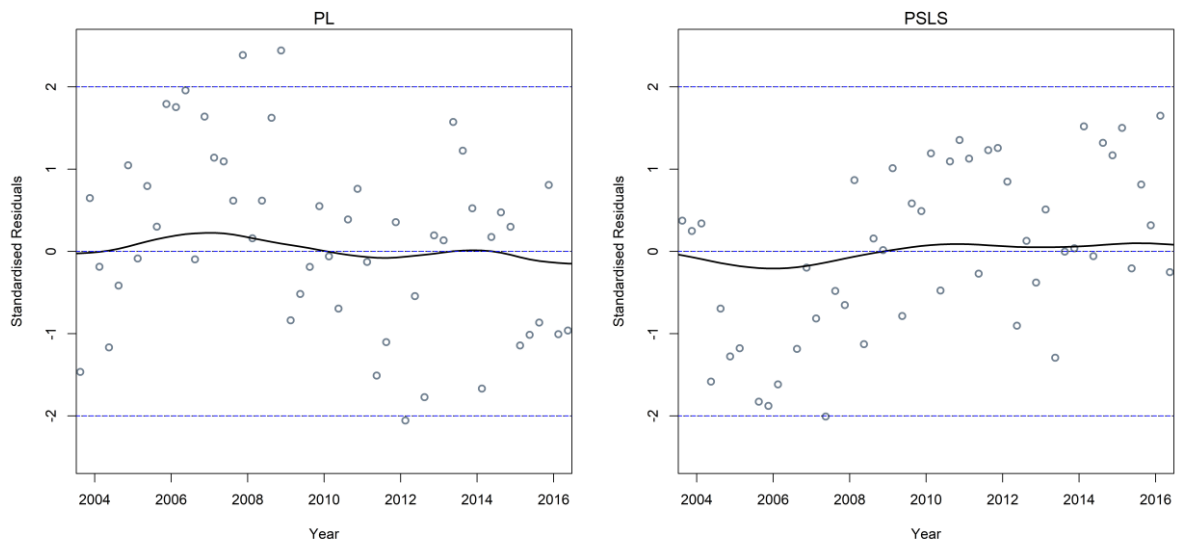


Figure 12: Standardised residuals from the fits to Maldives PL CPUE and the EU PS CPUE for the basic model.

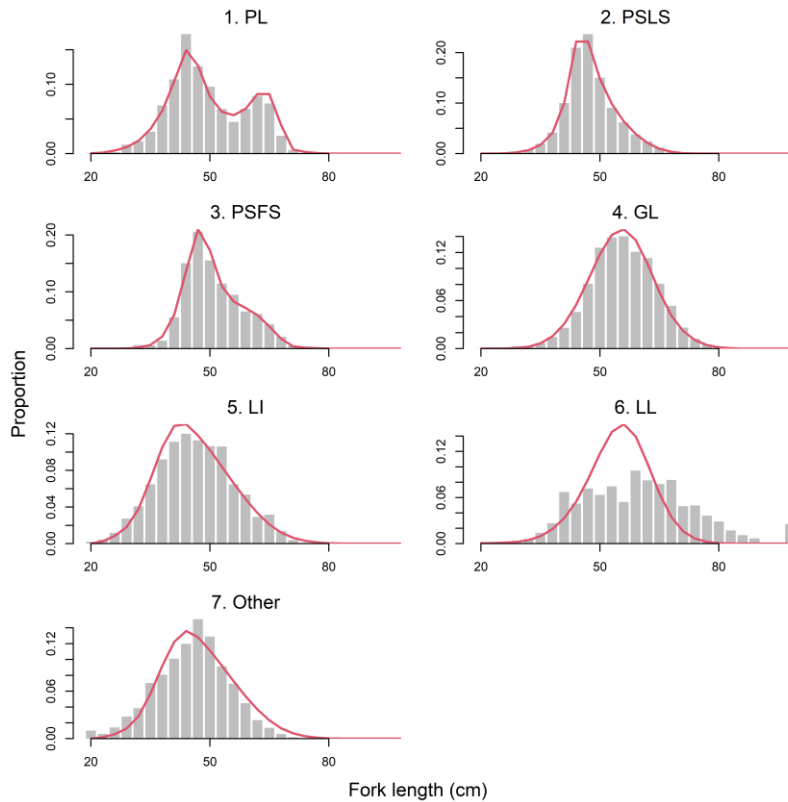


Figure 13: Observed (grey bars) and predicted (red line) length compositions (in 3 cm intervals) for each fishery of skipjack tuna aggregated over time for the basic model.

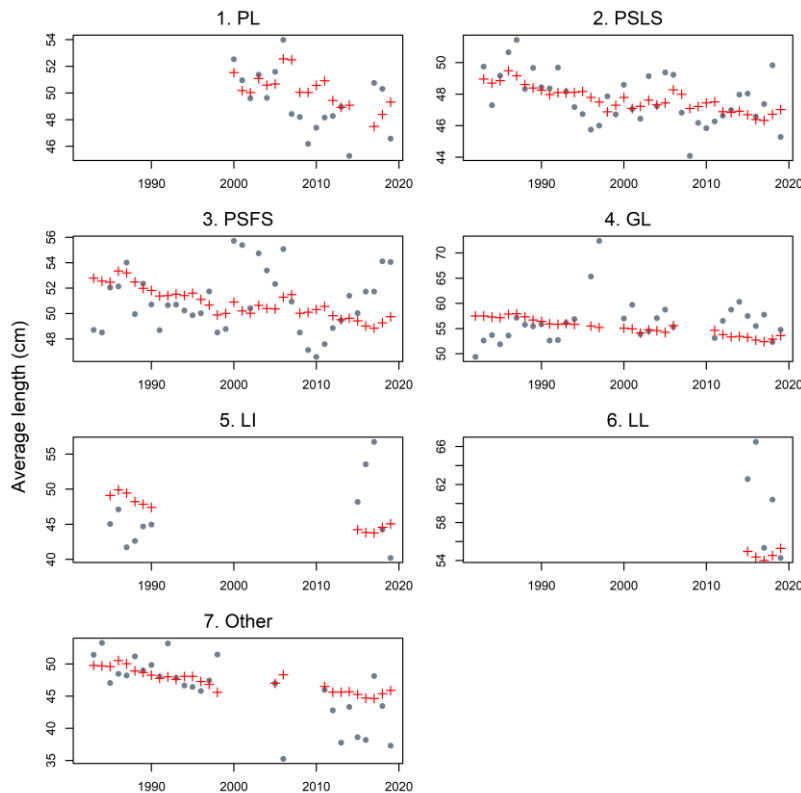


Figure 14: A comparison of the observed (grey points) and predicted (red points and line) average fish length (FL, cm) of skipjack tuna by fishery for the main fisheries with length data for the basic model.

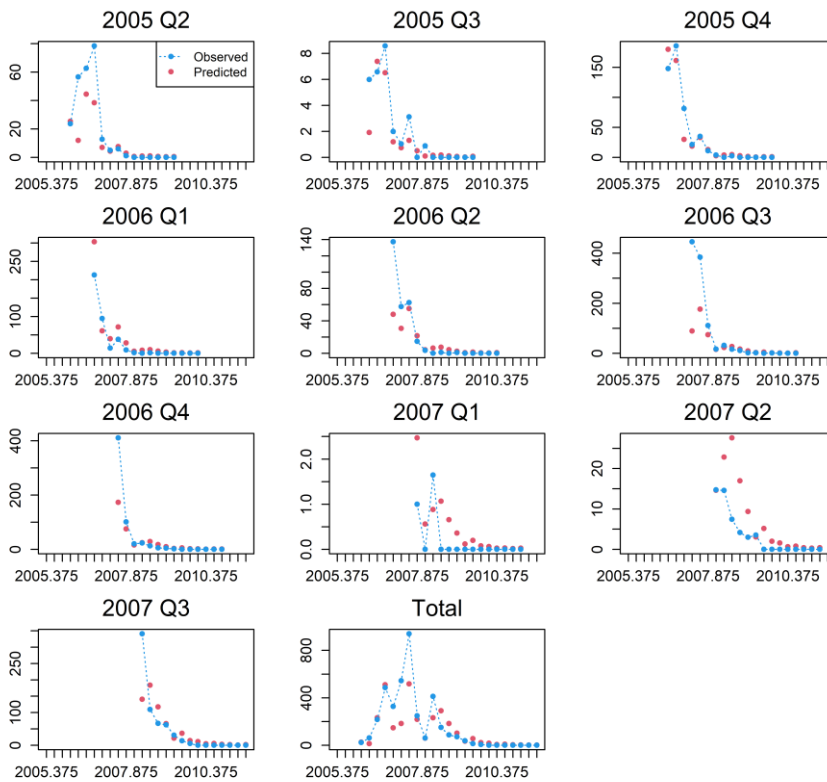


Figure 15: Observed and predicted the number of tag recoveries by the PSLS fishery by quarter following the mixing period from the basic model. Tag release groups represent the total releases in each quarter (aggregating the age groups that define individual release groups).

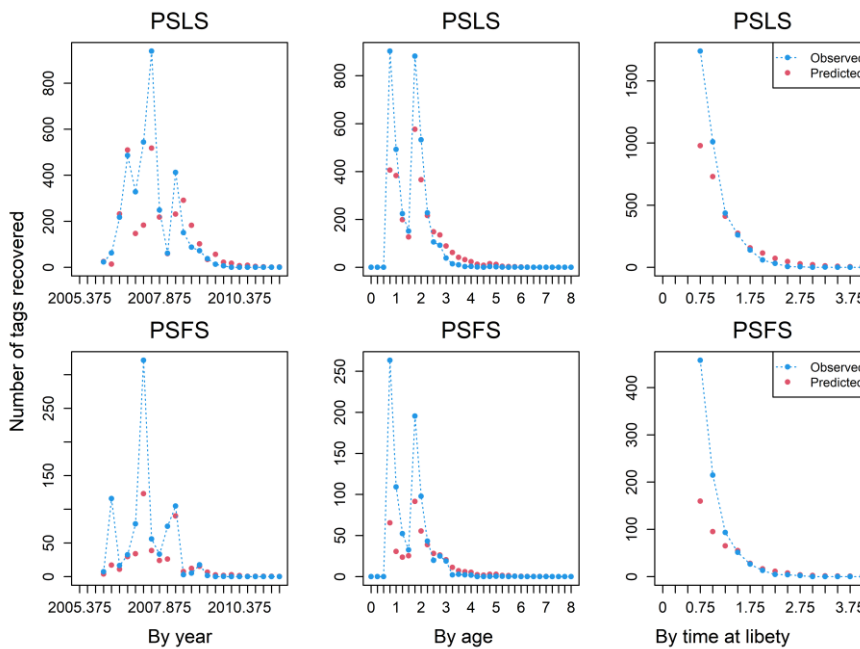


Figure 16: Observed and predicted number of tags recovered by year/quarter time-period (left), by age (mid), and by time at liberty (in quarters, right) for main recovery fisheries (PSLS and PSFS) from the basic model. Only tags at liberty after the four-quarter mixing period are included. Tag recoveries are aggregated for each fishery.

5.2.2 Model estimates

The selectivity estimates show that smaller fish (40–60 cm) are caught in the PSLS fishery, whereas larger fish are caught in the GI, LI, and LL fisheries and the youngest ages (including the 38cm maturity threshold) are only weakly vulnerable to the fisheries (Figure 17). The shape of the selectivity for the PL and PSFS reflects the multi-modal length distributions in the fisheries corresponding to a few younger and older age classes. The overall dome-shaped selectivity for most fisheries (except LL) could also be an artefact of the fixed M assumption, combined with the small number of observations of large fish, and uncertain growth curves.

Estimated annual recruitment has a standard deviation of about 0.3, which is commensurate with the assumed value of σ_R . Assuming larger values of σ_R did not change of the pattern nor increase the magnitude of the recruitment deviations, suggesting that the current assumption of σ_R did not impose excessive constraint on estimates of annual recruitment deviations, and that moderate variability is required to match the size composition and CPUE data. The periods of low recruitment correspond to the major decline in both the PL and PS CPUE indices and recent recruitment has been well above the historical average (Figure 18–left), driving the increase of the abundance index. Continuous spawning might be expected to cause important seasonal variability in recruitment for this species yet the model estimated recruitment in season 1–2 are consistently higher than season 3–4 (Figure 18–right), which may have been driven by the seasonal pattern in the CPUE data.

Estimated biomass showed two steep declines, one in the 1980 through to late 1990s and the other after the mid-2000s (Figure 19), which are explained by both catch removals and recruitment variability. The biomass has increased over the last five years from the historically low level. The fishing mortality rates were estimated to be high for PL, PSLS, and GI fisheries with significant increases since 2010 (Figure 20).

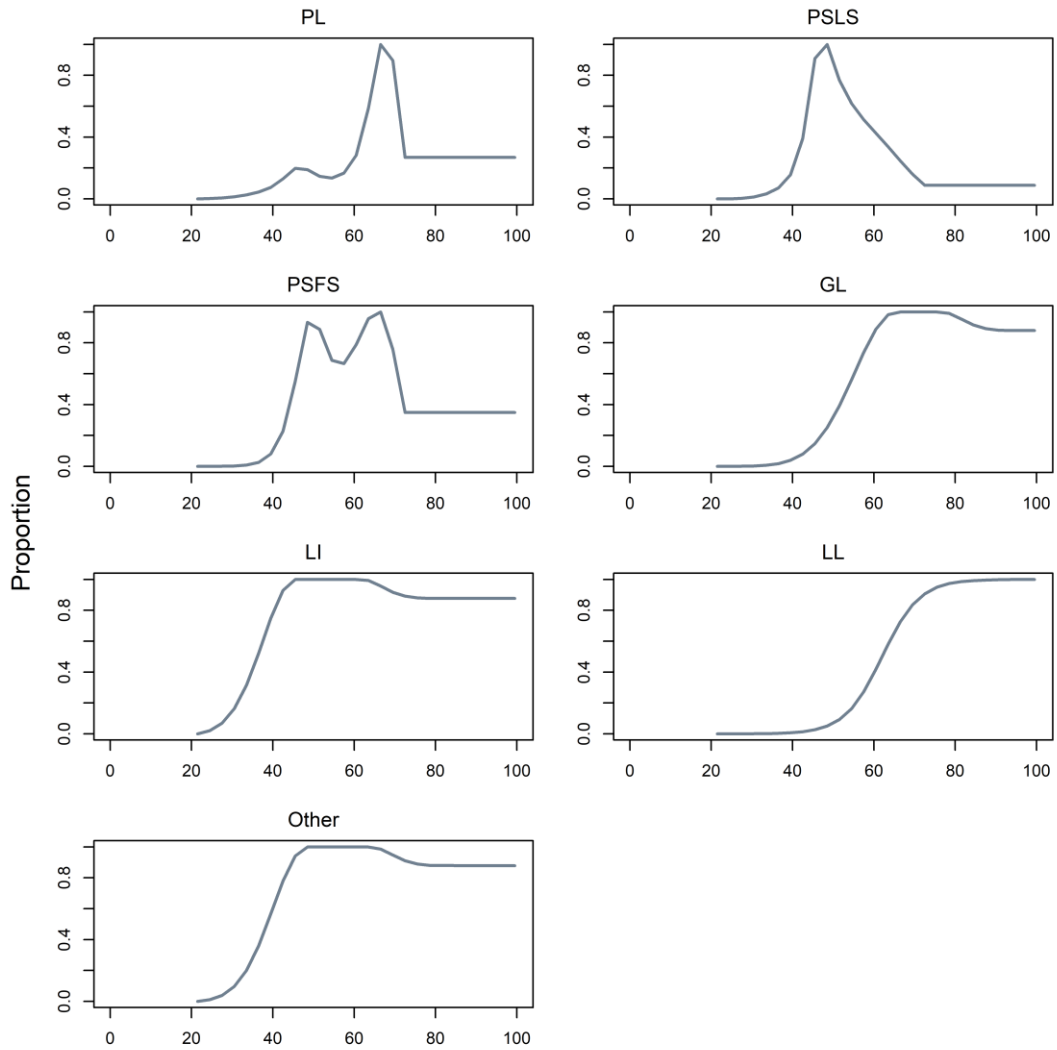


Figure 17: Length-based selectivity estimates by fishery for the basic model.

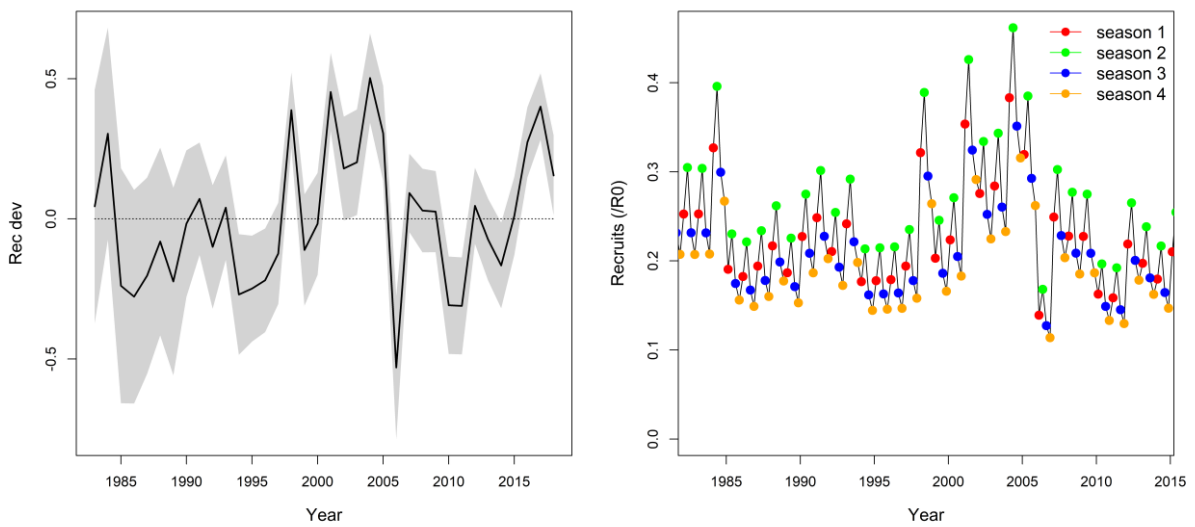


Figure 18: Estimated annual recruitment deviations (left) and recruits by season (right) for the basic model. The shaded area represents uncertainty estimates from the MPD fits.

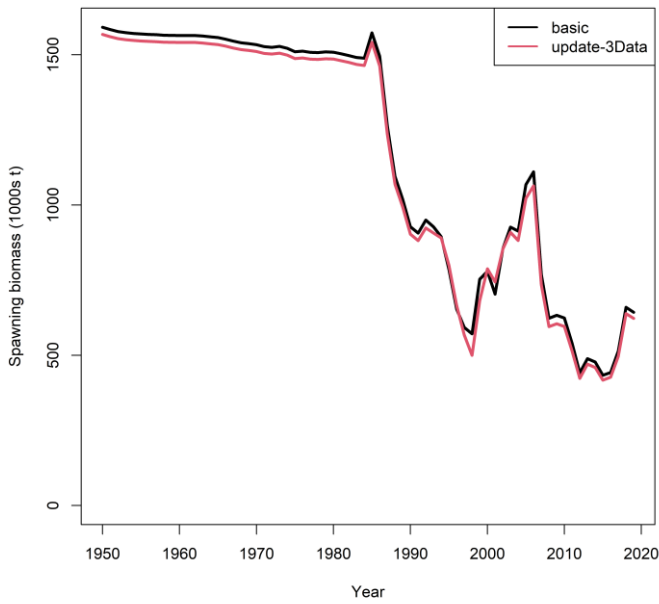


Figure 19: Estimated spawning biomass for the basic model (also showed the estimates from model update-3Data).

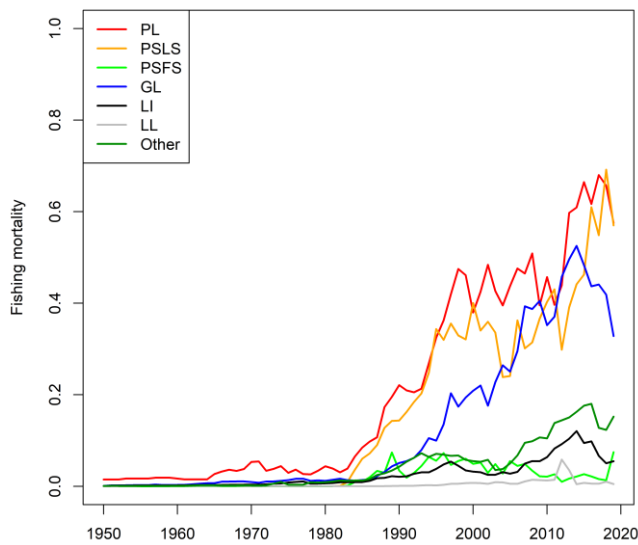


Figure 20: Trends in fishing mortality by fleet for the basic model.

5.3 Sensitivity models

Selected results from the sensitivity models are provided in Appendix B. Table B1 summarised the estimates of key model quantities. The estimated SSB_0 ranged from 1,324,830 to 2,179,790 t, target yield ranged from 383 738 t to 581 657 t, and current depletion ranged from 31% to 52%.

CPUE options

Despite of the overall consistency between the PL and PSLs index, they differed in the extent of implied stock depletion, with the PL index representing a larger decline in vulnerable abundance since mid-2000. Models fitting to the PL and PSLs index separately resulted estimated stock trends that are more in line with the respective index (Figure B1–a), and as expected, the model fitting to the PSLs index estimated a more optimistic stock abundance trend.

Extending the PL index back to 1975 (*PL1975*) caused a significant decline in estimated abundance in the late 1970s (Figure B1–B). The decline cannot be explained by the catch removal during that period (and was instead explained by an abnormally low level of recruitment). The drastic decline in the PL index in the 1970s is unlikely to have represented the level of depletion of skipjack tuna in the Indian Ocean given the small catch volume at the early stage of the fishery, and may have reflected local effects to various extent. The model fitting to the alternative PL index 1995 – 2018 (*PLoffset*) resulted a slightly lower abundance estimate (the fishing power offset term in the standardization appeared to have a larger effect on the early part of the time series, see Figure 3). It's worth noting that in both sensitivity models, the PSLs index was retained, which moderated the impact of the alternative PL index on the model.

Both the buoy-derived abundance index, and the index based on the associative dynamics with floating objects are fitted very well when included in the model (Figure B2), and the model estimates are very similar to the basic model (see Table B1). This is not surprising as both indices corroborate the increasing trend in the PSLs index over the last 5–8 years. However, as these indices are effectively based on skipjack tuna schools associated with the FADs, including them in the assessment model may over-weight the PSLs index.

A larger CV (0.2) did not have an appreciable impact on the model fits and the estimates of biomass trend are marginally more optimistic (Table B1). But the result is not conclusive and is conditional on other model configurations (e.g. weighting of the tagging data). From a biological point of view, a larger CV for the CPUE is probably more realistic, considering that both sets of indices are derived from catches of the younger population, which are influenced more by process errors (e.g. recruitment variability). From a modelling perspective, the use of a smaller CV allows a better fit to the CPUE and ensures stability of estimates in the context of a model grid. Traditionally the CPUE has also been given more confidence (and weight) than the tagging and size composition data in the skipjack assessment model.

Tagging program options

Model *rtss* included tag releases from both the RTTP and small-scale tagging program. The model included tag recoveries from both PS and PL fisheries, although the latter are not expected to contribute much to the model as the reporting rate from the PL fishery was estimated within the model. A tag mixing period of 2 quarter was assumed for this model, as less than 5% of tags were recovered after 2 quarters for the small-scale program. Despite of the shorter mixing period assumed, the model estimated a higher biomass throughout the model period (Figure B3 – a), with estimated SSB0 about 12% higher than the basic model. The estimate is likely to reflect the bias caused by the extreme low recovery rate of the small-scale tags by the PS fleet (~0.9% compared to the ~15% for the RTTP program). The fits to the recoveries for the small-scale tags were very poor. There are very few recoveries of SS tags from the main PSLs fisheries and there are no recoveries for many release groups at all (Figure B4 – a). For the PL recoveries, many RTTP release groups were recovered within a short time period, with clear evidence of overdispersion (Figure B4 – b).

There is conflict between the tag release/recovery data and the CPUE data, and the relative weighting of each data type influences the population scale parameter (R_0). Downweighting the tag data (10% and 1% of weight) yielded substantially higher level of stock biomass (Figure B3 – b), higher estimate of *target Yield (equilibrium catch at $F_{40\%SSB}$)* (Table B1). A likelihood profile analysis may provide further insights into the conflict between the CPUE and tag data.

Biological parameters

The longline fishery has extremely low catches of skipjack tuna, but they are included to provide size-based information. The LL fishery caught mostly large skipjack tuna and the right-hand side of the LL length distribution appeared to be poorly fitted. The LL catches of skipjack tuna is negligible and any bias in the LL selectivity is not expected to have any noticeable impact on the model. However, the lack of fits to the larger size classes may indicate that the assumed growth is probably not adequate. Increasing the variance of the length at age for the older fish (*growthCV*) improved the fits to the right-hand side of the LL length distribution marginally, and the model yielded a more pessimistic estimate of stock status (B5–a) (this model implied there were more large fish in the unfished population). However, there is lack of support in the tag release/recovery data for the larger variability assumed in this model (B6–a). Considering that the longline size samples are very unlikely to be representative of the fished population, and that the tag recoveries data are clearly inadequate in describing the growth for the older fish, further studies are required to better quantify the growth of skipjack tuna and its impact on the assessment model.

The basic model over-estimated the number of longer term tag recoveries from the older age classes (Figure 16), this could be an indication mis-specification of natural mortality. The sensitivity models suggested that estimates of longer-term tag recoveries can be improved by assuming higher *M* for older fish (Figure B6–b). On the other hand, assuming higher *M* for younger fish deteriorates the fits to tag recoveries of fish at liberty for the shorter term (Figure B6–b). Both sensitivity models reduced the biomass estimates for the early years but did not change the estimates in recent years (Figure B5–b).

Spatial structure

The two-area model (*io2*) assumes that the PL and PSLS CPUE index the vulnerable abundance in the eastern and western IO respectively. The area structure allows the model to account for the heterogeneous population trend and consequently improves the fits to the CPUE (Figure B8). The model estimated similar initial spawning biomass in both regions but the eastern IO has a much higher depletion (Figure B9). The model estimated a migration rate that increases with age from the western to the eastern region. This is probably an artefact of the variability and trend in the CPUE data, as there is no explicit information on migration (the tag release and recovery data are confined to the western region). There appears some improvement in the fits to the tag data in the main recovery phase (Figure B10), as the model allows for some local dynamics of the tag release/recovery process (rather than assuming they are from one homogenous population). The two-area model estimated a higher stock abundance than the one area model (Figure B7–a), because tags were assumed to be mixed within the western population rather than the whole IO. The conflict between the tagging data and the CPUE appears to have been alleviated in the two-area model– down-weighting of tagging data within the two-area model (*io2TagLambda01*) had a lesser effect on estimated abundance than the one area model (see Figure B7–a and B3).

Temporal structure

The basic model was re-configured as the CSMY structure. The sensitivity model (Q4) estimated a very similar stock abundance 1950 – 2019 (See Figure B7-b). This confirmed that both model structures are very close in modelling most of the seasonal population processes. A more detailed comparison of between the two temporal model structures can be found in Fu (2017).

5.4 Final model options

The two-area model provides an alternative yet plausible spatial representation of the IO skipjack population. The two-area model setting has yielded different estimates of stock trend and productivity to the one-area model. The spatial structure contributes to an importance source of uncertainty and therefore is included in the final model options.

A key conclusion from the sensitivity analysis is that the tagging data conflicts with the CPUE and the model estimates are sensitive to the weighting of the tagging data. Thus, the final model options included two different weighting assumptions on the tagging data set. The weightings were applied by the values assigned to the proportion (λ) of the two components of the tag likelihood included in the total model likelihood.

The final model options also included three alternative values of steepness of the BH SRR (h 0.7, 0.8 and 0.9). These values are considered to encompass the plausible range of steepness values for skipjack tuna.

The period of tag mixing is another source of uncertainty. Analysis of tagging data tend to suggest that at least 3 or more quarters is required for the assumption of homogeneous mixing to be reasonably valid. There are so few tag recoveries with a time of liberty exceeding 5 so that longer mixing periods probably do not contain much useful information. The final model options thus included a mixing period of 3 or 4 quarters.

The final model ensemble corresponds to a full combination of two spatial structures, three steepness values, two levels of tag weighting, and two tag mixing period assumptions, with a total of 24 models (see Table 5). These models encompass a wide range of stock trajectories (Figure 21). Across the model grid, initial spawning biomass (SSB₀) ranged from 1 515 250 to 2 141 300 t, current depletion ranged from 38% to 51% (SSB₂₀₁₉/SSB₀) (Table 6). In general, higher stock biomass are associated with low weighting of tagging data, longer tag mixing period, and a lower steepness value. The weighting of the tagging data had a much bigger impact on the biomass estimates in the spatially aggregated models (Figure 21)

Table 6: Maximum Posterior Density (MPD) estimates of the main stock status indicators from individual models from final model options.

	SB_0	SB_{TGT}^*	SB_{2019}	SB_{2019}/SB_0	SB_{2018}/SB_{TGT}	F_{2018}/F_{TGT}^{**}	F_{TGT}^{**}	$Yield_{TGT}^{***}$
io_h70_t3_rttp_tlambda01	2 141300	856 534	1 026 720	0.48	1.20	0.89	0.89	518 554
io_h70_t3_rttp_tlambda1	1 704200	681 694	655 768	0.38	0.96	1.30	1.31	427 183
io_h70_t4_rttp_tlambda01	2 195170	878 084	1 073 020	0.49	1.22	0.85	0.85	530 251
io_h70_t4_rttp_tlambda1	1 780 350	712 155	720 127	0.40	1.01	1.20	1.21	442 154
io_h80_t3_rttp_tlambda01	2 031 130	812 467	1 002 080	0.49	1.23	0.83	0.83	545 496
io_h80_t3_rttp_tlambda1	1 591 390	636 569	642 962	0.40	1.01	1.20	1.21	442 357
io_h80_t4_rttp_tlambda01	2 084 160	833 677	1 046 610	0.50	1.26	0.79	0.79	558 322
io_h80_t4_rttp_tlambda1	1 668 080	667 244	704 165	0.42	1.06	1.12	1.12	459 482
io_h90_t3_rttp_tlambda01	1 955 190	782 091	985 726	0.50	1.26	0.78	0.78	569 433
io_h90_t3_rttp_tlambda1	1 515 250	606 110	634 482	0.42	1.05	1.13	1.14	456 680
io_h90_t4_rttp_tlambda01	2 007 600	803 053	1 029 110	0.51	1.28	0.75	0.75	583 226
io_h90_t4_rttp_tlambda1	1 591 740	636 709	693 585	0.44	1.09	1.05	1.05	475 472
io2_h70_t3_rttp_tlambda01	2 098 470	839 395	931 104	0.44	1.11	0.95	0.95	521 844
io2_h70_t3_rttp_tlambda1	1 991 570	796 635	846 575	0.43	1.06	1.20	1.04	497 688
io2_h70_t4_rttp_tlambda01	2 108 040	843 225	938 713	0.45	1.11	0.94	0.94	524 096
io2_h70_t4_rttp_tlambda1	1 984 840	793 945	841 310	0.42	1.06	1.08	1.05	494 121
io2_h80_t3_rttp_tlambda01	1 995 790	798 323	917 070	0.46	1.15	0.88	0.88	549 152
io2_h80_t3_rttp_tlambda1	1 863 280	745 320	813 607	0.44	1.09	1.11	0.98	515 081
io2_h80_t4_rttp_tlambda01	2 004 670	801 875	923 936	0.46	1.15	0.87	0.87	551 506
io2_h80_t4_rttp_tlambda1	1 866 980	746 800	817 368	0.44	1.09	1.08	0.98	514 058
io2_h90_t3_rttp_tlambda01	1 924 920	769 974	907 995	0.47	1.18	0.82	0.82	573 320
io2_h90_t3_rttp_tlambda1	1 742 850	697 146	767 332	0.44	1.10	1.04	0.96	522 126
io2_h90_t4_rttp_tlambda01	1 933 380	773 360	914 446	0.47	1.18	0.82	0.82	575 783
io2_h90_t4_rttp_tlambda1	1 784 500	713 807	800 605	0.45	1.12	1.01	0.93	531 700

* $SS_{40\%SSB}$ ** $F_{40\%SSB}$ *** $Yield_{F40\%SS}$

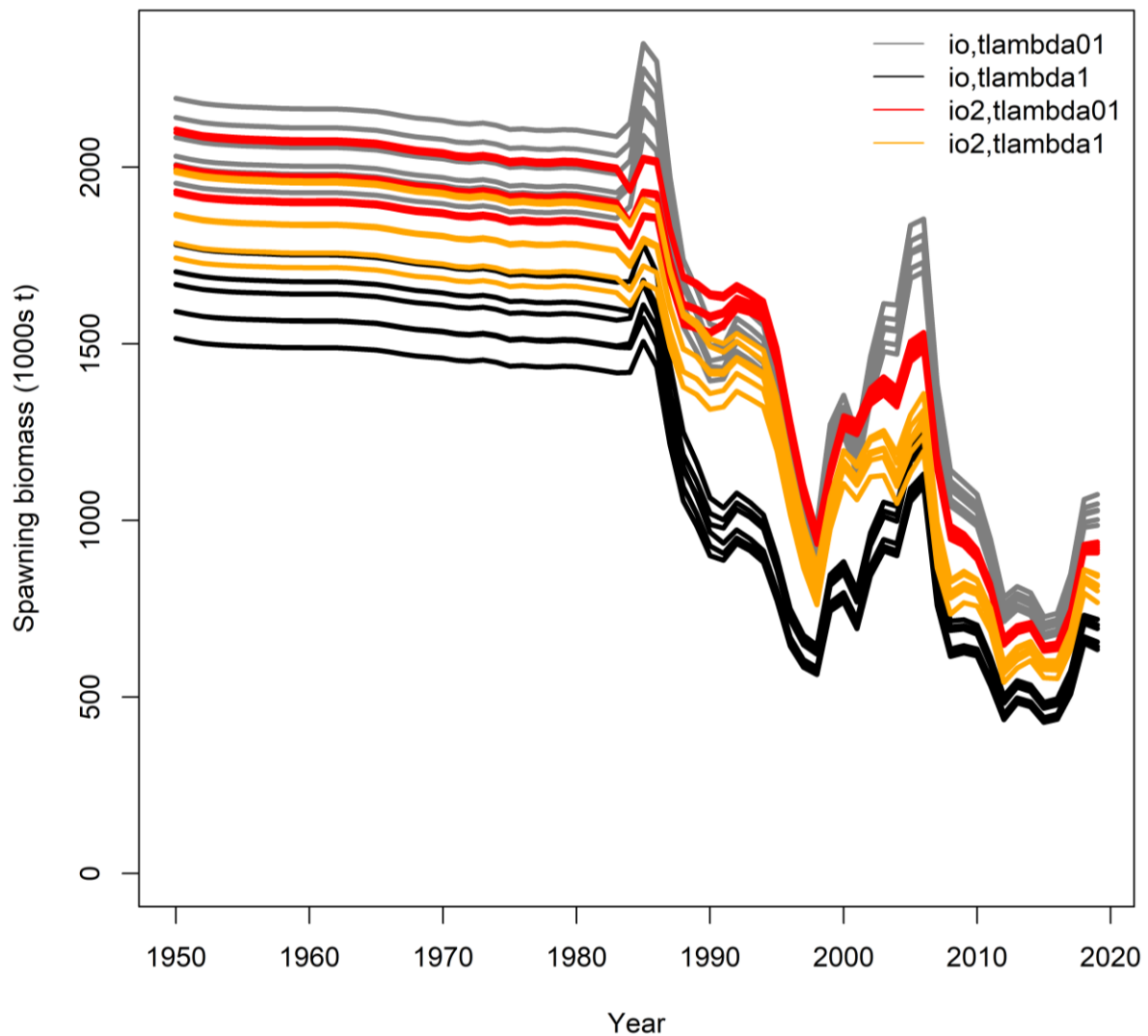


Figure 21: Spawning biomass trajectories from the final model options (details in Table 5)

5.5 Diagnostics

Several diagnostic tools were run for the basic model, including likelihood profiling, retrospective, and hindcasting analysis. Further diagnostics using the “run” test (a tool developed by Henning Winker and Felipe Carvalho to evaluate random or systematic pattern in the residuals.) was performed to the sensitivity model ‘io2’ and the results are provided in Appendix C.

5.5.1 Profile likelihood

The profile likelihood on R_0 for the basic model confirmed that the global minimum was obtained by the maximum likelihood estimate (Figure 22 – left), which was further supported by a jittering analysis. However, it suggested that there are conflicts between the abundance indices, size frequency, and tagging data. The size data appears to support a higher R_0 (i.e. higher B_0), the abundance data favours a low R_0 , and tag data supports an even lower R_0 . Further breakdown of the likelihood components suggested that the length composition from the main fisheries (i.e. PL and PSLS) appears to be consistent with the total likelihood, providing both the upper and lower bounds for R_0 , whereas fisheries

that mostly caught mostly large fish (i.e. LL, GI, LI) provide no constrain on the upper bound for R_0 (Figure 22 – right). The average fish length in the PL and PSLs fisheries showed a declining trend whereas it remained relatively stable in the GI and LI fisheries (see Figure 14). Nonetheless, under the current weighting (i.e., effective sample size), the overall influence of the length composition on the stock estimates appears small, as indicated by an aged structured production model analysis (Maunder & Piner 2015).

The assumption that tags are fully mixed with the skipjack population is likely a cause of data conflict. The quality and representativeness of length samples from some fisheries (e.g. LL, LI, GI, etc.) is a concern. Attempts to address the data conflict focused mostly on evaluating the impact of data weighting on the model. For the final models, a smaller CV (e.g. 0.1) was assigned to the CPUE, considering that more confidence (and weight) should be given to the CPUE data. The size data was down weighted with sample sizes constrained to a maximum of 10, to prevent undue influence on abundance estimates, while allowing reasonable estimates of selectivity and fits to the size distributions. The spatial partitioning alleviated the violation of the tag mixing assumption at the ocean-basin scale. The final model options also included alternative tag likelihood lambda values to account for the uncertainty arising from the conflict between the tagging and CPUE data.

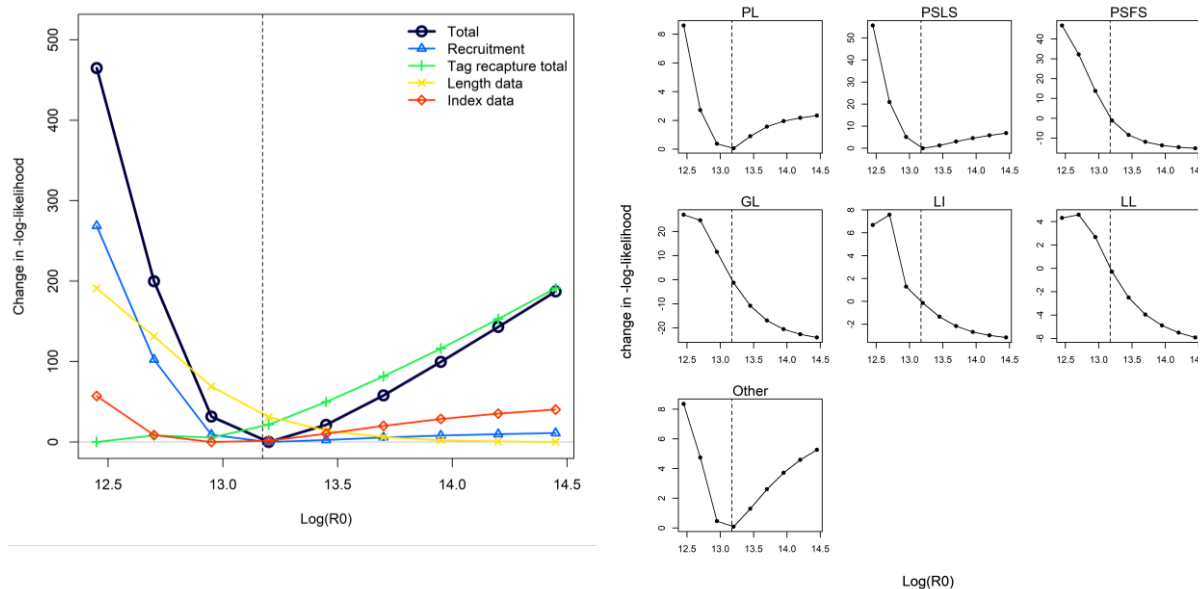


Figure 22: Likelihood profile including total and component likelihood function values (left), and the likelihood profile for the length data by fleet (right), for the basic model.

5.5.2 Retrospective analysis

Retrospective analysis is a diagnostic approach to evaluate the reliability of parameter and reference point estimates and to reveal systematic bias in the model estimation. It involves fitting a stock assessment model to the full dataset. The same model is then fitted to truncated datasets where the data for the most recent years are sequentially removed. The retrospective analysis was conducted to the reference model for the last 5 years of the assessment time horizon to evaluate whether there were any strong changes in results. The analysis involves sequentially removing 4 quarters of data at each trial.

The analysis conducted to the basic model indicated there is a minor retrospective pattern for SSB related indicators (e.g. reduced SSB estimates as data was sequentially removed). Further investigations showed the retrospective pattern was due to the influence of the size data from a number fisheries (see Section 5.5.1). Isolating the influence of these size data in the last few years will eliminate the retrospective pattern. Overall, the retrospective pattern appears insignificant, which provided some confidence on the robustness of the model.

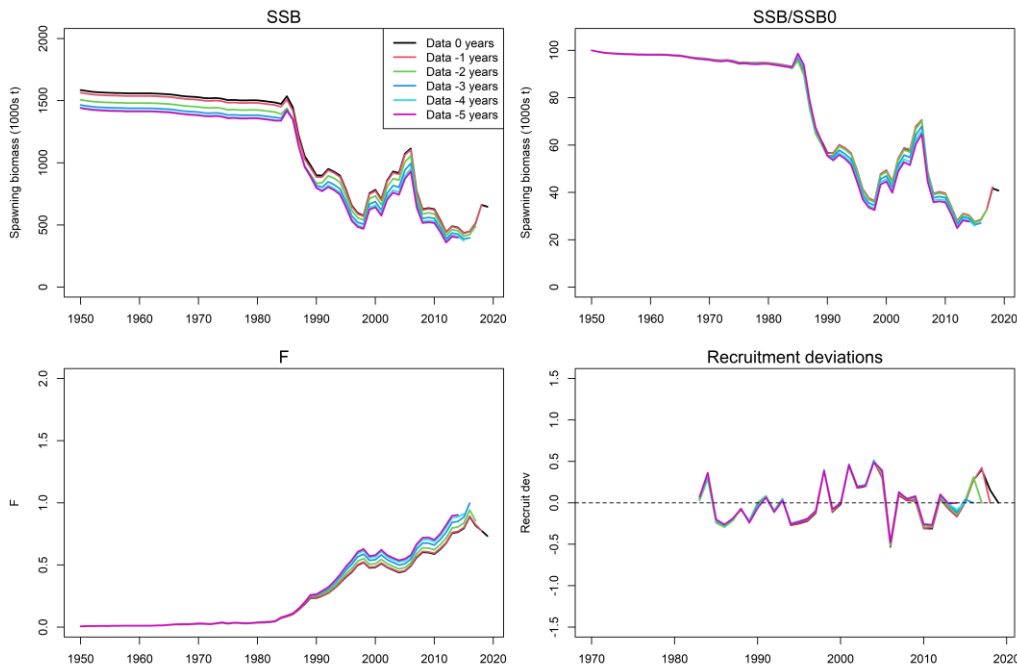


Figure 23: Retrospective analysis summary for the basic model. Each panel shows estimates of key indicators from models with data sequentially removed for 1 – 5 years.

5.5.3 Hindcasting analysis

Retrospective analysis evaluates model’s stability with respect to recent data. The Hindcasting analysis (Kell et al. 2016) further assesses the model’s predictive power by making forward projections of the CPUE index using truncated models (i.e. models were fitted with data sequentially removed and were projected forward with catches added back in). The Hindcasting diagnostics were provided for the basic model using the ‘ss3diags’ package (Winker et al. 2019). The results suggested reasonable stability with respect to the model’s predictive capability.

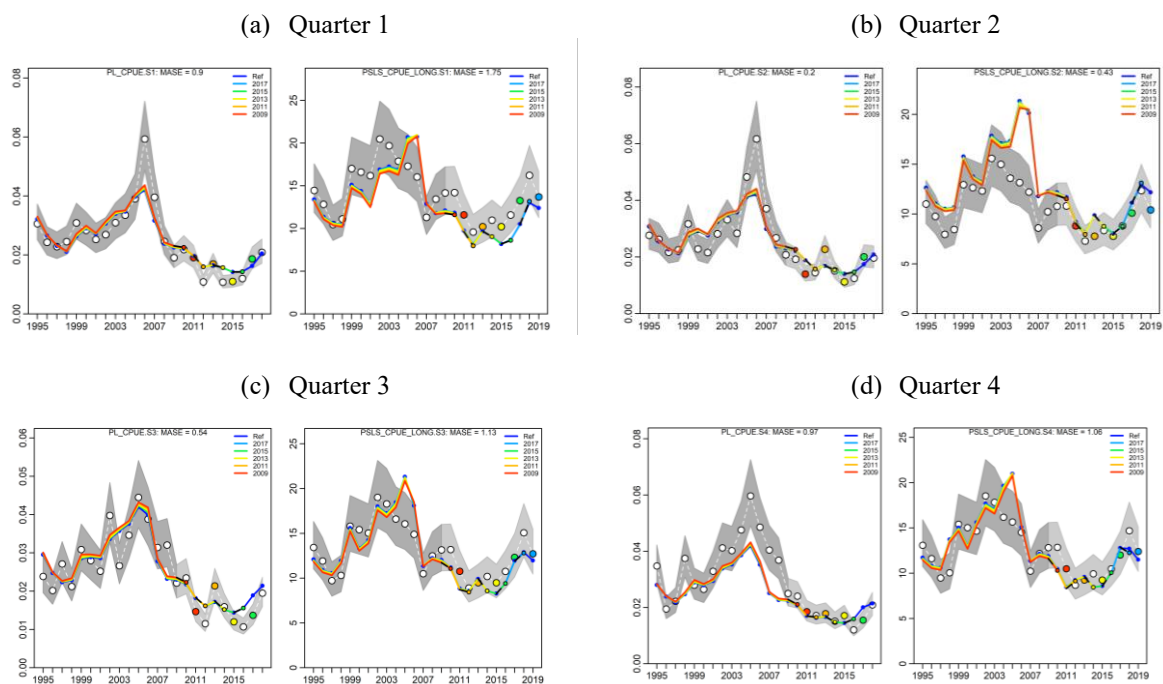


Figure 24: The Hindcasting analysis summary for the basic model: each panel shows the predicted quarterly CPUE index (PL and PSLS) from models with data sequentially removed for 2, 4, 6, 8, 10 years.

6. STOCK STATUS

6.1 Current status and yields

Estimates of stock status were determined for the final model options, including alternative assumptions on spatial structure, alternative values of SRR steepness, tag mixing period, and the alternative weighting of the tag data. Stock status was determined for individual models (Table 6), as well as the for all (24) models combined, incorporating uncertainty of each model based on estimated variance-covariance matrix of parameters (Table 7).

Depletion-based reference points (see Section 3.5) were derived based on the average F-at-age matrix in 2019, representing the most recent pattern of exploitation from the fishery. For the selected model options, point estimates of $Yield_{40\%SSB_0}$ ranged from 445 000 t to 586 000 t (Table 6). Models with higher steepness generally yielded comparatively higher estimates of target yield. Annual catches over the last five years the 1990s have been within the range of the estimated target yield (Figure 25).

In general, current stock biomass relative to the *depletion*-based benchmarks are not fundamentally different for the range of model options. Averaging across the model grid, fishing mortality rates have been increasing rapidly since 1980, and has decreased slightly over the last few years (Figure 25). Biomass was estimated to have declined considerably in the 1980s, again in the mid-2000s, but have increased since 2010 (Figure 25).

Estimates were combined across from the 24 models to generate the KOBE stock status plot (Figure 26). For individual models, the uncertainty is characterised using the multivariate lognormal Monte-Carlo approach (Walter et al. 2019, Walter & Winker 2019, Winker et al. 2019), based on the maximum likelihood estimates and variance-covariance of F/F_{TGT} and SSB/SSB_{TGT} . Thus, estimates of stock status included both within and across model uncertainty. Combined across the model ensemble, SSB_{2019} was estimated to be of 1.13 SSB_{TGT} (0.98–1.28), and F_{2019} was estimated 0.98 F_{TGT} (0.75–1.21) (Table 7). The probability of the stock being in the green Kobe quadrant in 2019 is estimated to be about 63%. The stock is therefore considered not to be overfished and is not subject to overfishing in 2019.

Table 7: Estimated Status of skipjack tuna in the Indian Ocean from the model ensemble.

Catch in 2019:	547 248
Average catch 2015–2019:	506 554
Yield _{40%SSB} (1000 t) (80% CI):	515 (445–586)
MSY (1000t) (80% CI)	574 (477–671)
F _{40%SSB}	0.60 (0.53–0.66)
SB ₀ (1000 t) (80% CI):	1900 (1614–2191)
SB ₂₀₁₉ (1000 t) (80% CI):	854 (632–1077)
SB _{40%SB0}	759 (641–877)
SB _{20%SB0}	350 (320–438)
SB ₂₀₁₉ /SB ₀ (80% CI):	0.45 (0.40–0.50)
SB ₂₀₁₉ / SB _{40%SB0}	1.13 (0.98–1.28)
SB ₂₀₁₉ / SB _{MSY}	2.01 (1.45–2.58)
F ₂₀₁₉ / F _{40%SB0}	0.98 (0.75–1.21)
F ₂₀₁₉ / F _{MSY}	0.55 (0.31–0.78)

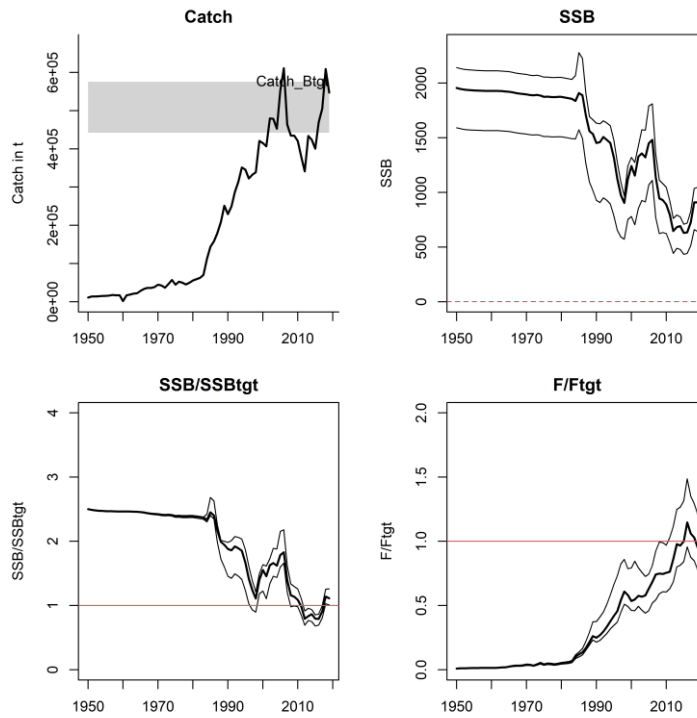


Figure 25: Estimated stock trajectories for the Indian Ocean skipjack from the final model grid. Thin black lines represent 5%, 50%, 95% percentiles. In the catch plot, dotted lines represent estimate of Yield_{40%SSB}, the shaded area represents 5th and 95th percentiles. SSBtgt refers to SB_{40%SSB0} and Ftgt refers to F_{40%SSB0}.

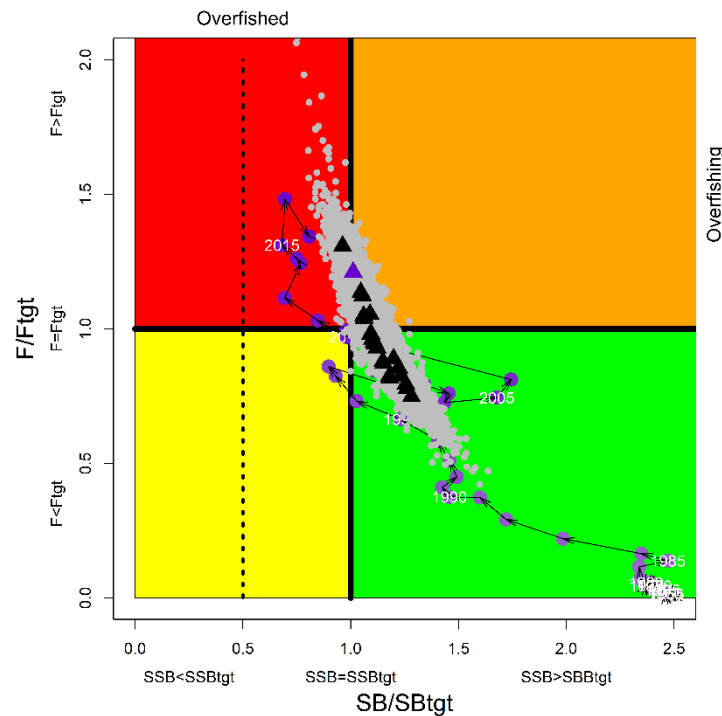


Figure 26: current stock status, relative to SB_{40%SSB0} (x-axis) and F_{40%SSB0} (y-axis) reference points for the final model grid, as well as time series of historical stock status for the basic model. Triangles represent MPD estimates from individual models. Grey dots represent uncertainty from individual models. The dashed lines represent limit reference points for IO skipjack (SB_{lim} = 20%SSB₀).

7. DISCUSSION

This report presents a preliminary stock assessment for Indian Ocean skipjack using a sex-aggregated, age-structured Stock Synthesis model. It represents an update and revision of the 2017 assessment model with newly available information, including updated and revised CPUE indices and length composition data. There are no fundamental changes in the structure of the assessment model compared to the previous assessment (Fu 2017), with the revisions mostly concerning the refinement of the fleet structure. A basic model was configured to assess the model performance. A range of sensitivity models were explored to assess the impact of key data sets and model assumptions. The final model options involved running a combination of configuration and model settings related to the spatial structure, stock-recruitment steepness, tag data weighting, and tag mixing period. These model options are thought to have contributed to the main source of uncertainty associated with estimates of stock dynamics and productivity. The final estimates of stock status are based on a model grid of 24 models, incorporating uncertainty estimates from both within and across the model ensemble.

The overall stock status estimates obtained from the range of model options do not differ substantially from the previous assessment. Considering the quantified uncertainty, spawning stock biomass in 2019 was estimated to be 45% of the unfished levels and thus was above the target level ($SSB_{2019}/SSB_{TGT} = 1.13$). Current fishing mortality was estimated to be lower than the target fishing mortality ($F_{2019}/F_{TGT} = 0.98$). The retrospective analysis provided some confidence on the robustness of the model with respect to recent data.

The Indian Ocean skipjack fisheries present a number of problems in the development of a stock population model: there is considerable uncertainty on growth, natural mortality, and recruitment; there are good time series of CPUE, but their reliability to track abundance is highly uncertain, given that the CPUE were derived from regional fisheries; there is a large amount of data on size structure, but the sampling were unlikely to be truly random; the tagging data are very informative but the key assumption of homogeneous mixing is unlikely to be met. As with earlier assessments, the models presented here, while fairly representing some of the data (e.g., the biomass indices), also show some signs of poor fit. The assessment examined various combinations of assumptions to explore the sensitivity and describe the uncertainty in the stock status. It is unlikely that the estimates of historical stock size are accurate, given assumptions about annual recruitment, the reliance on the historical catch-effort indices of abundance, and the conflicts between key observational datasets. Current stock status as estimated here should thus be treated with caution.

The inclusion of the tagging data in the assessment model is contingent upon the assumption of homogeneous mixing i.e. that tagged and untagged individuals are equally vulnerable to exploitation. Independent analyses of RTTP tag data have shown strong evidence of poor mixing for 3 quarters, but proper mixing might never occur at the basin scale (IOTC–WPTT19). It was recognized that the mixing problem may positively bias the biomass estimate, but the effects of the mixing problem in the RTTP-IO data are not easy to predict. Several approaches were considered. Firstly, the small-scale tagging data were thought to be useful in increasing spatial coverage and providing further insights into spatial dynamics. Yet there is more evidence that small scale tag data are likely to be mixed mostly with the local population (relatively high recovery by the PL fishery within a short period and extremely low recovery by the PSLS fishery). The small-scale data further suffer the problem of high tag losses and low and variable reporting rates. Secondly spatial disaggregation (the two-area model) confines the tag dynamics to the western region only and the partition was thought be well fitted with the geographical scale of the observed skipjack (Sharma et al. 2012, Fonteneau 2014). Yet the complete mixing of tags within the western Purse Seine fish population might never occur either. If that is the case, finer partition of the model region (such as the four-area stratification proposed by Fonteneau (2014)) may be worth pursuing. Thirdly, the down-weighting of tagging data, albeit arbitrary, allows the uncertainty arising from the conflict between the tagging data and other abundance indices to be incorporated into the assessment results to some extent.

There is good rationale to support the introduction of spatial dimension within the assessment model. In addition to the heterogeneity in tag mixing, the spatial disaggregation better accounts for differential regional depletion, improves the overall model fits (see the diagnostics of the io2 model in Appendix C), and potentially reduces the bias induced by an aggregated model. However, the additional complexity introduced by the spatial structure requires more data support which the model is probably lacking (e.g. restricted tag releases and limited recovery across region boundary is not very informative of movement or migration). As the regional CPUE were derived from different fisheries, there is lack of information to link the respective CPUE indices among regions, undermining the power of the model to estimate the relative level of biomass among regions. Fu (2017) did not find a credible range of regional biomass distribution under a wider range of model options for the spatially structured model. Given these uncertainties, the spatially disaggregated model requires further development and improvement.

There are also several progresses on the development of CPUE indices for skipjack tuna. The longer time series of the Maldivian indices provide valuable information to verify the relative abundance in the period during the industrialisation of the fishery beginning in the 1980s, and serve to discriminate the degree to which short term population fluctuations are due to fishery depletion or recruitment variability. Innovative echo buoy indices and the index based on associative behaviour and acoustic data provide some confidence on the credibility of the recent abundance trend derived from the purse seine catch effort data. Abundance indices from other fisheries seem unlikely at this stage. the PSFS CPUE is not considered to be representative of SKJ stock biomass because of the highly peculiar occurrence of SKJ in the free school fishery and free schools of skipjack have dramatically decreased over time (Gaertner et al. 2017). Longline CPUE is not indicative of SKJ abundance in general, given the the erratic patterns in reported catch, effort and CPUE.

Based on estimates of the assessment, the stock is considered not to be overfished and is not subject to overfishing in 2019. However, the very recent fishing mortality rates were above the target and catches have exceeded the range of the estimated target yield. The high productivity and life history characteristics of skipjack tuna (fast growing, early maturation, high fecundity and high M) suggest that this species is resilient and not easily prone to overfishing (ISSF 2012). The PS indices show a large increase of abundance in the large years. The increase in PS FAD CPUE are associated with declining catch rate in the free schools. This could be a result of school fragmentation (Fonteneau and Marsac 2016), which hypothesized that the growing number of drifting FADs could have partitioned biomass from free schools. This is in contrast with some of the early analysis which suggested declining trend based on indicators of PS fishery, including declining SKJ catches for purse seiners and baitboats, declining percentages and catch rates of SKJ in FAD schools, reduced average weight of SKJ (Marsac et al. 2017, Fonteneau and Marsac 2016, Fonteneau 2014). An analysis of the correlation between the annual size of favourable habitat for feeding, the annual nominal catch rates and the total catches of skipjack agrees with the near full exploitation of skipjack in the IO since the 2000s (Druon, et al. 2016).

8. ACKNOWLEDGMENTS

Thanks to the many people that contributed to the collection of this data historically, analysts involved in the CPUE standardization, and developers for providing the SS3 software, Henning Wicker for providing the ss3diags package.

9. REFERENCES

- Adam, M.S. 2010. Declining catches of skipjack in the Indian Ocean – observations from the Maldives. IOTC-2010-WPTT-09.
- Baidai, Y., Dagorn, L., Amande, M.J., Kaplan, D., Gaertner, D., Deneubourg, J.L., Capello, M. 2020. Assessing tropical tuna populations from their associative behaviour with floating objects: A novel abundance index for skipjack tuna (*Katsuwonus pelamis*) in the Western Indian Ocean. IOTC-2020-WPTT22(DP)-13.
- Chassot, E., Assan, C., Esparon, J., Tirant, A., Delgado d, Molina, A., Dewals, P., Augustin, E., Bodin, N. 2016. Length-weight relationships for tropical tunas caught with purse seine in the Indian Ocean: Update and lessons learned. IOTC-2016-WPDCS12-INF05.
- Chassot, E., Floch, P., Dewals, V., Fonteneauc, R., Pianet. 2010. Statistics of the main purse seine fleets fishing in the Indian Ocean, 1981-2009. IOTC-2010-WPTT-13.
- Dammannagoda, S.T., Hurwood, D.A., Mather, P.B. 2011. Genetic analysis reveals two stocks of skipjack tuna (*Katsuwonus pelamis*) in the northwestern Indian Ocean. *Can. J. Fish. Aquat. Sci.* 68: 210-223.
- Delgado de Molina, A., Areso, J.J., Ariz, J. 2010. Statistics of the purse seine Spanish fleet in the Indian Ocean (1984-2009). IOTC-2010- WPTT-19.
- Druon, J.N., Chassot, E., Murua, H., Soto, M. 2016. Preferred feeding habitat of skipjack tuna in the eastern central Atlantic and western Indian Oceans: relations with carrying capacity and vulnerability to purse seine fishing. IOTC-2016-WPTT18-31.
- Eveson, J.P. 2011. Preliminary application of the Brownie-Petersen method to skipjack tag-recapture data. IOTC-2011-WPTT-13-31Rev_1
- Eveson, J.P., Million, J., Sardenne, F., Le Croizier, G. 2012. Updated Growth estimates for Skipjack, Yellowfin And Bigeye Tuna in the Indian Ocean using the most recent Tag-Recapture and Otolith data. IOTC-2011-WPTT-14-23Rev_1
- Fontenea. A. 2014. On the movements and stock structure of skipjack (*Katsuwonus pelamis*) in the Indian ocean. IOTC-2014-WPTT16-36.
- Fonteneau, A., Marsac, F. 2016. Fishery indicators suggest symptoms of overfishing for the Indian Ocean skipjack stock. IOTC-2016-WPTT18-INF02, 15p.
- Gaertner, D., Katara, I., Billet, N., Fonteneau, A., Lopez, J., Murua, H., Daniel, P. 2017. Workshop for the development of Skipjack indices of abundance for the EU tropical tuna purse seine fishery operating in the Indian Ocean. 17-21 July 2017. AZTI, Spain.
- Gaertner, D., Hallier, J.P. 2014. Tag shedding by tropical tunas in the Indian Ocean and other factors affecting the shedding rate. *Fish. Res.* (2014).
- Grande, M., Murua, H., Zudaire, I., Korta, M. 2010. Spawning activity and batch fecundity of skipjack, *Katsuwonus pelamis*, in the Western Indian Ocean. IOTC-2010-WPTT-47.
- Grewe, P.M., Wudianto, C.H., Proctor, M.S., Adam, A.R., Jauhary, K., Schafer, D., Itano, K., Evans, A., Killian, S., Foster, T., Gosselin, P., Feutry, J., Aulich, R., Gunasekera, M., Lansdell C.R. Davies. 2019. Population Structure and Connectivity of Tropical Tuna Species across the Indo Pacific Ocean Region. WCPFC-SC15-2019/SA-IP-15.

Guery, L., Aragno, V., Kaplan, D., Grande M., Baez, J.C., Abascal, F., Urunga J., Marsac, F., Merino, G. and Gaertner, D. 2020. Skipjack CPUE series standardization by fishing mode for the European purse seiners operating in the Indian Ocean. IOTC-2020-WPTT22(DP)-12.

Hallier, J.P., Million, J. 2009. The contribution of the regional tuna tagging project – Indian Ocean to IOTC stock assessment. IOTC-2010-WPTT-24.

Hillary, R.M., Million, J., Anganuzzi, A., Areso, J.J. 2008a. Tag shedding and reporting rate estimates for Indian Ocean tuna using double-tagging and tag-seeding experiments. IOTC-2008-WPTDA-04.

Hillary, R.M., Million, J., Anganuzzi, A., Areso, J.J. 2008b. Reporting rate analyses for recaptures from Seychelles port for yellowfin, bigeye and skipjack tuna. IOTC-2008-WPTT-18.

Hoyle, S.D., Leroy, B.M., Nicol, S.J., Hampton, J. 2015. Covariates of release mortality and tag loss in large-scale tuna tagging experiments. *Fisheries Research* 163, 106-118.

IOTC 2016. RESOLUTION 16/02. ON HARVEST CONTROL RULES FOR SKIPJACK TUNA IN THE IOTC AREA OF COMPETENCE. IOTC RESOLUTION 16/02.

IOTC 2020. Review of the Statistical Data and Fishery Trends for Tropical Tunas. IOTC-2020-WPTT22(DP)-08.

IOTC-WPTT19 2017. Report of the 19th Session of the IOTC Working Party on Tropical Tunas. Seychelles, 17–22 October 2017. IOTC-2017-WPTT19-R[E]: 118 pp.

IOTC-WPTT22(DP) 2020. Report of the 22nd Session of the IOTC Working Party on Tropical Tunas. Online, 22 - 24 June 2020. IOTC-2020-WPTT22(DP)-R[E]: 35 pp

ISSF 2011. Report of the 2011 ISSF stock assessment workshop. Technical Report ISSF Technical Report 2011-02, Rome, Italy, March 14-17, 2011.

ISSF 2012. Stock Status Ratings, 2012: Status of the world fisheries for tuna. ISSF Technical Report 2012-04B. International Seafood Sustainability Foundation, Washington, D.C., USA.

Itano, D. 2000. The reproductive biology of yellowfin tuna (*Thunnus albacares*) in Hawaiian waters and the western tropical Pacific Ocean: Project summary. JIMAR Contribution 00-328 SOEST 00-01.

Jauharee, A.R., Adam, M.S. 2009. Small Scale Tuna Tagging Project – Maldives 2007 Project Final Report - October 2009. Marine Research Centre, Malé 20-025, Republic of Maldives. Unpublished report, 17p.

Kayama, S., Tanabe, T., Ogura, M., Okamoto, H. and Y. Watanabe. 2004. Daily age of skipjack tuna, *Katsuwonus pelamis* (Linnaeus), in the eastern Indian Ocean. IOTC-2004-WPTT-03.

Kiyofuji, H., Aoki, Y., Kinoshita, J., Ohashi, S., Fujioka, K. 2019. A conceptual model of skipjack tuna in the Western and Central Pacific Ocean (WCPO) for the spatial structure configuration. WCPFC-SC15-2019/SA-WP-11.

Kell, L.T., Kimoto, A., Kitakado, T., 2016. Evaluation of the prediction skill of stock assessment using hindcasting. *Fisheries research*, 183, pp.119-127.

- Kolody, D., Herrera, M., Million, J. 2011. Indian Ocean Skipjack Tuna Stock Assessment 1950-2009 (Stock Synthesis). IOTC-2011-WPTT13-31_Rev1.
- Kolody, D., Eveson, J.P., Preece, A.L., Davies, C.R., Hillary, R.M. 2018. Recruitment in tuna RFMO stock assessment and management: A review of current approaches and challenges. Fisheries Research Volume 217, 217-234.
- Langley, A. 2016a. Stock assessment of bigeye tuna in the Indian Ocean for 2016 — model development and evaluation. IOTC-2016-WPTT18-20
- Langley, A. 2016b. An update of the 2015 Indian Ocean Yellowfin Tuna stock assessment for 2016. IOTC-2016-WPTT18-27
- Maunder, M.N., Piner, K.R., 2015. Contemporary fisheries stock assessment: many issues still remain. ICES J. Mar. Sci. 72, 7–18, <http://dx.doi.org/10.1093/icesjms/fsu015>.
- McKechnie, S. Hampton, J., Pilling, G. M., Davies N. 2016. Stock assessment of skipjack tuna in the western and central Pacific Ocean. WCPFC-SC12-2016/SA-WP-04.
- Mohamed, S. 2007. A bioeconomic analysis of Maldivian skipjack tuna fishery. M.Sc. thesis, University of Tromso. 39 pp.
- Marsac, F., Fonteneau, A., Lucas, J., Báez, J., Floch, L. Data-derived fishery and stocks status indicators for skipjack tuna in the Indian Ocean Floch. IOTC-2017-WPTT19-09.
- Murua, H., Kitakado, T., Mosqueira, I., Adam, S., Merino, G., Fu, D., Bentley, N. 2017. Calculation of Skipjack Catch Limit for the Period 2018-2020 Using the Harvest Control Rule Adopted in Resolution 16/02. IOTC-2017-SC20-12 Rev_1
- Medley, P., Ahusan, M., Adam, M.S. 2020. Bayesian Skipjack and Yellowfin Tuna CPUE Standardisation Model for Maldives Pole and Line 1970-2019. IOTC-2020-WPTT22(DP)-11
- Methot Jr, R.D., Wetzel, C.R. (2013) Stock synthesis: A biological and statistical framework for fish stock assessment and fishery management. Fisheries Research, 142(0): 86-99.
- Methot Jr, R.D., Taylor, I.G., Doering, K. 2020. 2020. Stock Synthesis User Manual Version 3.30.15. U.S. Department of Commerce, NOAA Processed Report NMFS-NWFSC-PR-2020-05.
- Nishikawa, Y., Honma, M., Ueyanagi, S., Kikawa, S. 1985. Average distribution of larvae of oceanic species of scombrid fishes, 1956–1981. Far Seas Fisheries Research Laboratory, Shimizu. S Series 12. WPTT-04-06.
- Santiago, J., Uranga, J., Quincozes, I., Grande, M., Murua, H., Merino, G., Urtizberea, A., Zudaire, I. Boyra, G., 2020. Novel Index of Abundance of Skipjack in The Indian Ocean Derived from Echosounder Buoys. IOTC-2020-WPTT22(DP)-14.
- Sharma, R., Herrera, M., Million, J. 2012. Indian Ocean Skipjack Tuna Stock Assessment 1950-2011 (Stock Synthesis). IOTC-2012-WPTT14-29 Rev-1.
- Sharma, R., Herrera, M., Million, J. 2014. Indian Ocean Skipjack Tuna Stock Assessment 1950-2013 (Stock Synthesis). IOTC-2014-WPTT16-43 Rev_3.
- Wujdi, A., Setyadji, Bram., Nugroho, S. C. 2017. Preliminary stock structure study of skipjack tuna (katsuwonus pelamis) from south java using otolith shape analysis. IOTC-2017-WPTT19-xx.

Walter, J., Hiroki, Y., Satoh, K., Matsumoto, T., Winker, H., Ijurco, A.U., Schirripa, M., 2019. Atlantic bigeye tuna stock synthesis projections and kobe 2 matrices. Col. Vol. Sci. Pap. ICCAT 75, 2283–2300.

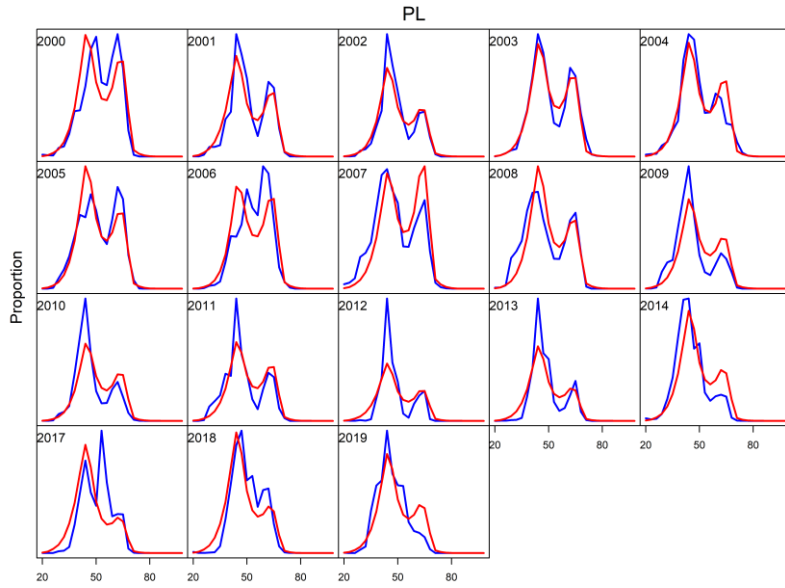
Walter, J., Winker, H., 2019. Projections to create Kobe 2 Strategy Matrices using the multivariate log-normal approximation for Atlantic yellowfin tuna. ICCAT-SCRS/2019/145 1–12.

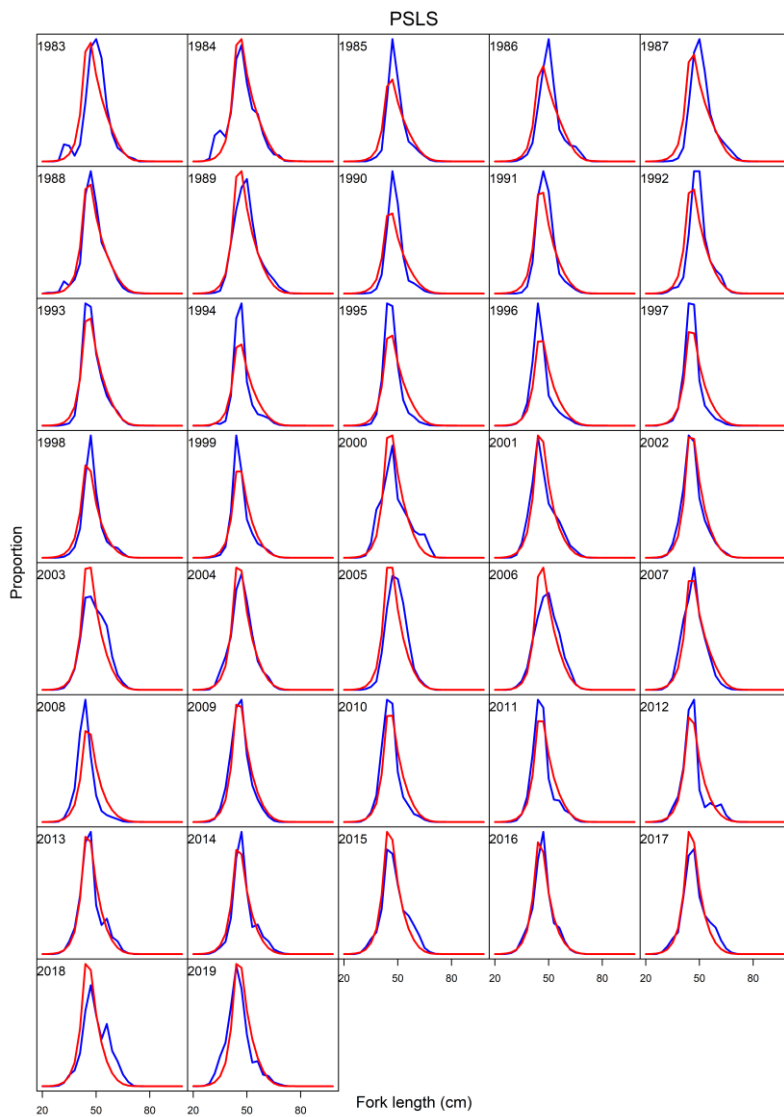
Winker, H., Walter, J., Cardinale, M., Fu, D. 2019. A multivariate lognormal Monte-Carlo approach for estimating structural uncertainty about the stock status and future projections for Indian Ocean Yellowfin tuna. IOTC–2019–WPTT21–51.

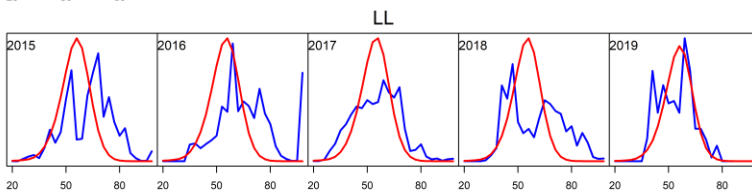
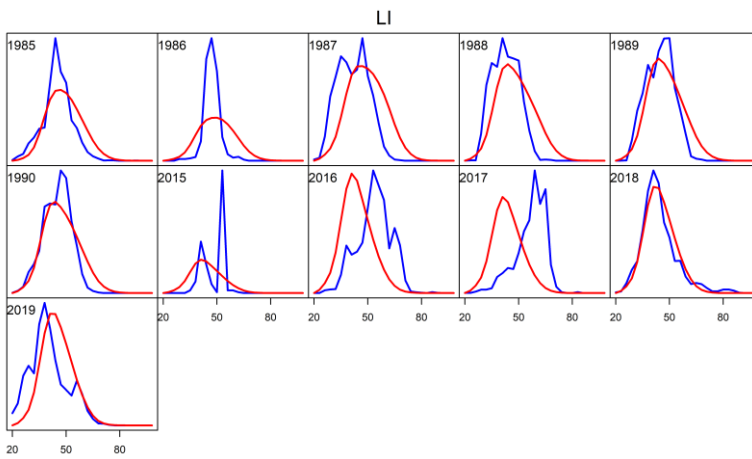
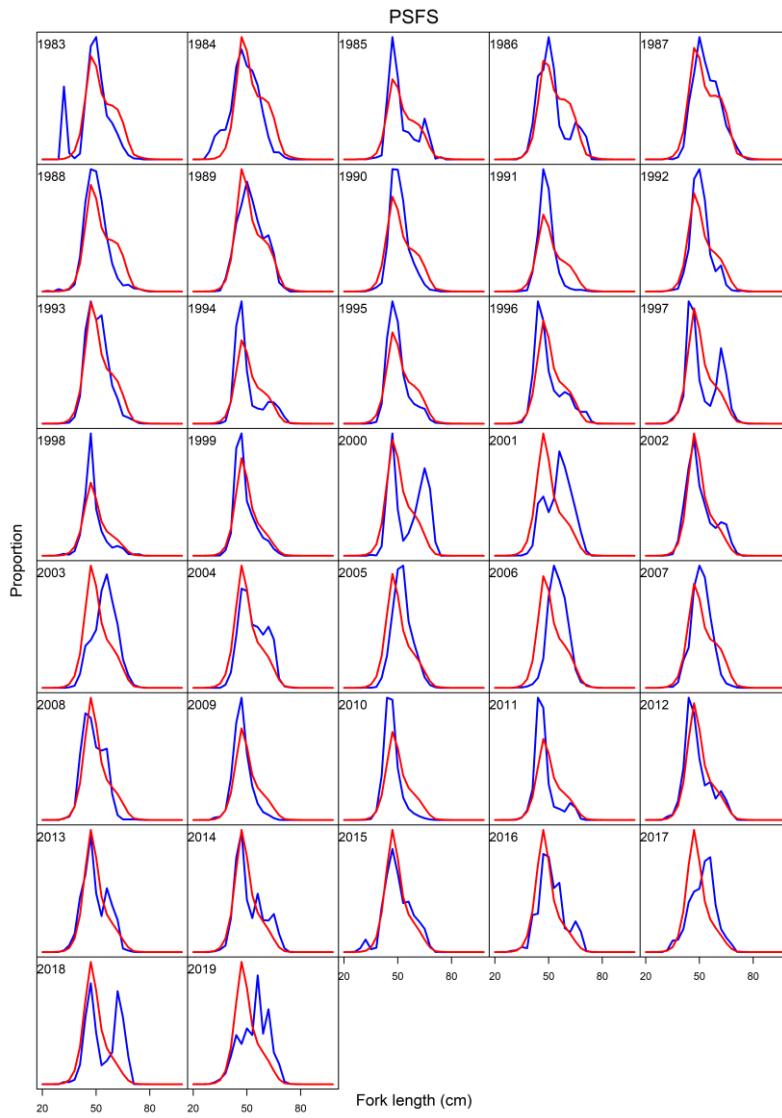
Winker, H., Carvalho, F., Cardinale, M., Kell, K. 2020. ss3diags. R package version 1.0.2.

Vincent, M. T., Pilling, G.M., J Hampton, J. 2019. Stock assessment of skipjack tuna in the western and central Pacific Ocean. WCPFC-SC15-2019/SA-WP-05-Rev2.

APPENDIX A: FITS TO LENGTH DATA FOR MAIN FLEETS FROM THE BASIC MODEL







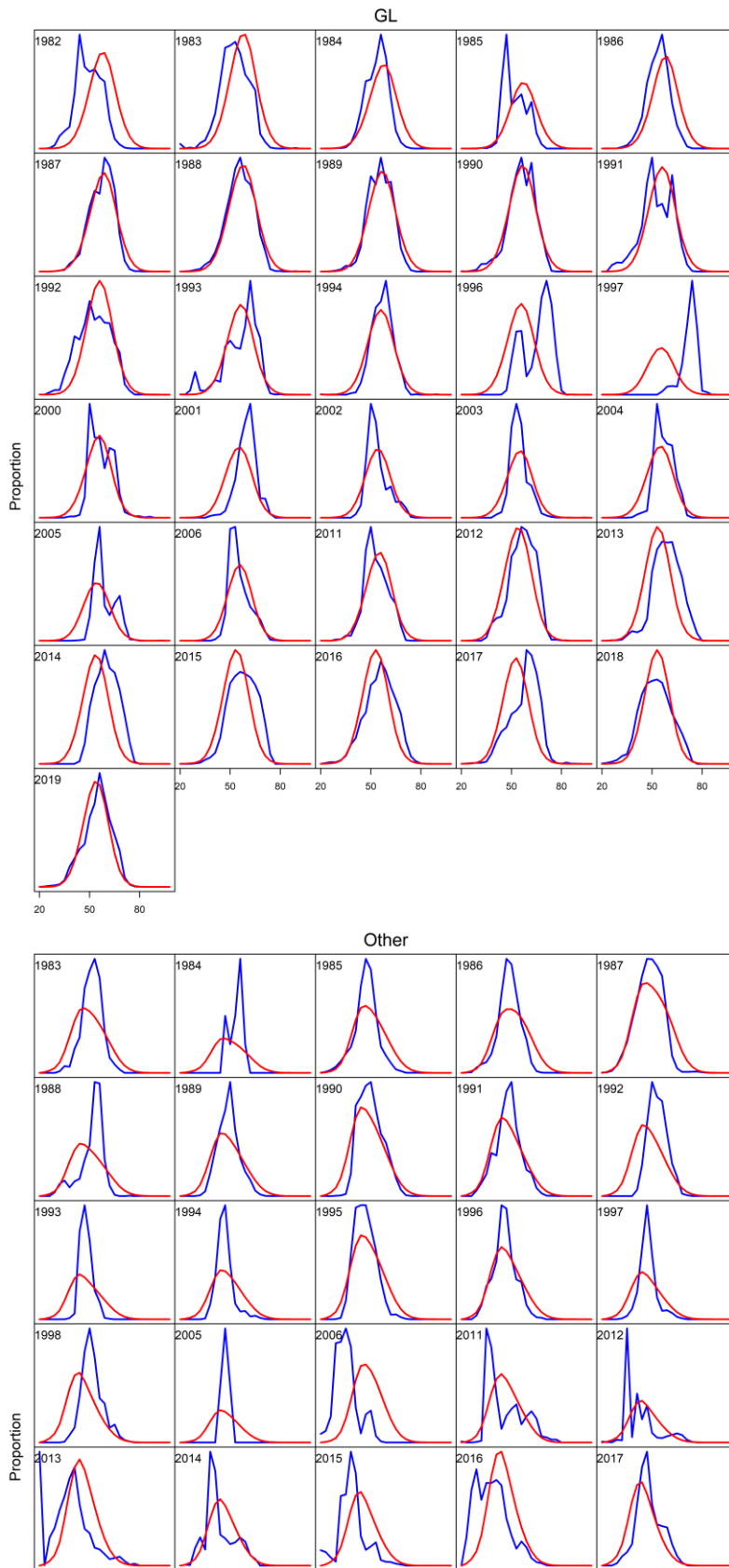


Figure A1: Observed (blue) and predicted (red) length compositions for the PL, PSLS, PSFS, GI, LI, LL, and Other fisheries by year for the basic model.

APPENDIX B: SELECTED RESULTS FROM THE SENSIVITY MODELS

Table B1. Maximum Posterior Density (MPD) estimates of the main stock status indicators from the sensitivity model options. SB

	SB_0	SB_{TGT}^*	SB_{2019}	SB_{2019}/SB_0	SB_{2018}/SB_{TGT}	F_{2018}/F_{TGT}^{**}	$Yield_{TGT}^{***}$
<i>basic</i>	1 591 390	636 569	642 962	0.40	1.01	1.01	442 357
<i>PL</i>	1 495 440	598 180	465 458	0.31	0.78	0.78	414 719
<i>PSLS</i>	1 787 980	715 200	839 548	0.47	1.17	1.17	485 632
<i>PL1975</i>	1 420 790	568 331	644 519	0.45	1.13	1.13	396 473
<i>Ploffset</i>	1 555 340	622 148	587 230	0.38	0.94	0.94	439 202
<i>BAI</i>	1 633 130	653 264	679 080	0.42	1.04	1.04	451 160
<i>Cv20</i>	1 642 910	657 164	650 345	0.40	0.99	0.99	452 241
<i>growthCV</i>	1 395 390	558 166	428 462	0.31	0.77	0.77	383 738
<i>MhighJ</i>	1 395 000	557 982	670 352	0.48	1.20	1.20	522 986
<i>MhighA</i>	1 324 830	529 948	645 216	0.49	1.22	1.22	518 063
<i>rtss</i>	1 766 390	706 569	811 598	0.46	1.15	1.15	484 548
<i>tagLambda01</i>	2 031 130	812 467	1 002 080	0.49	1.23	1.23	545 496
<i>tagLambda001</i>	2 179 790	871 929	1 127 040	0.52	1.29	1.29	581 657
<i>Q4</i>	1 664 740	665 897	688 084	0.41	1.03	1.03	437 320
<i>io2</i>	1 863 280	745 320	813 607	0.44	1.09	1.09	515 081
<i>io2tagLambda01</i>	1 995 790	798 323	917 070	0.46	1.15	1.15	549 152

* 40%SSB

** $F_{40\%SSB}$ *** $Yield_{F40\%SSB}$

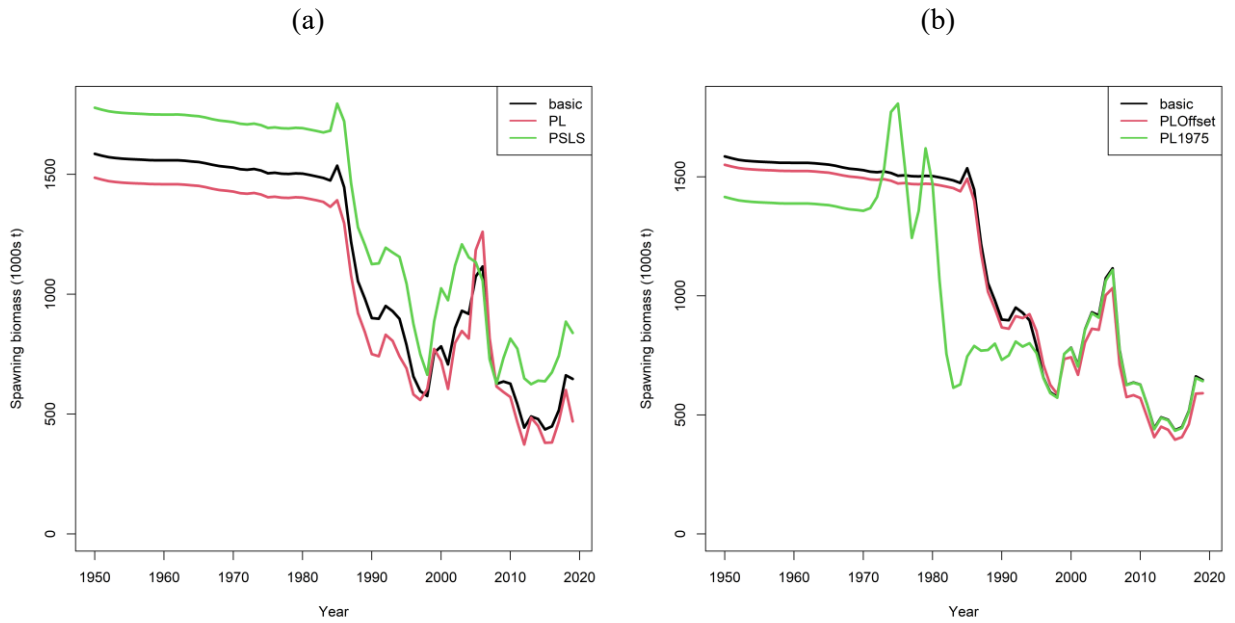


Figure B1: A comparison of estimated spawning biomass from sensitivity models related to CPUE options – (a) model PL and PSLS (b) model PLOffset and PL1975. A description of the sensitivity models is given in.

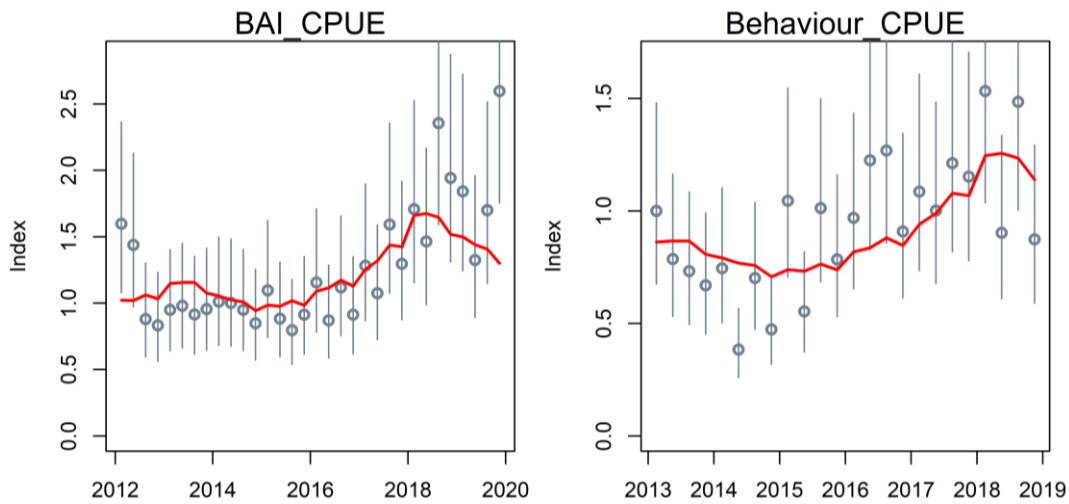


Figure B2: Fits to the Purse seine buoy-derived abundance index (left), and the index based on the associative dynamics with floating objects and acoustic data (right), from the sensitivity model BAI (see Table 4). The fits to PL and PSLS indices are not shown here.

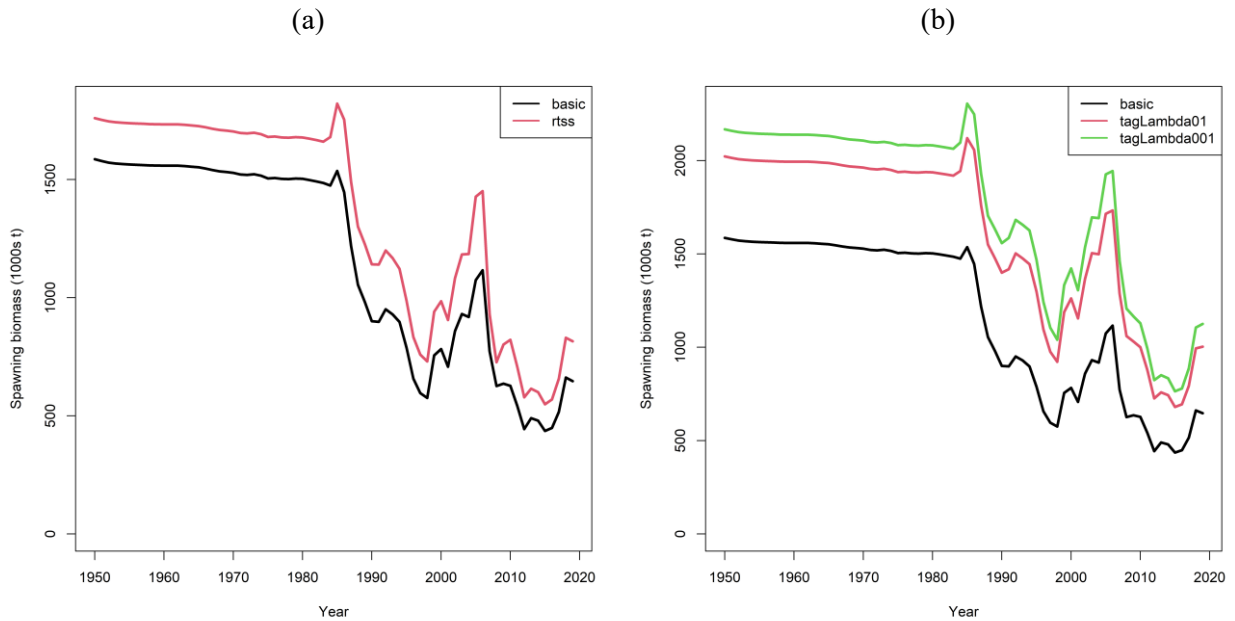


Figure B3: A comparison of estimated spawning biomass from sensitivity models related to tag options – (a) model *rtss* (b) model TagLambda001 and TagLambda01. A description of the sensitivity models is given in Table 4.

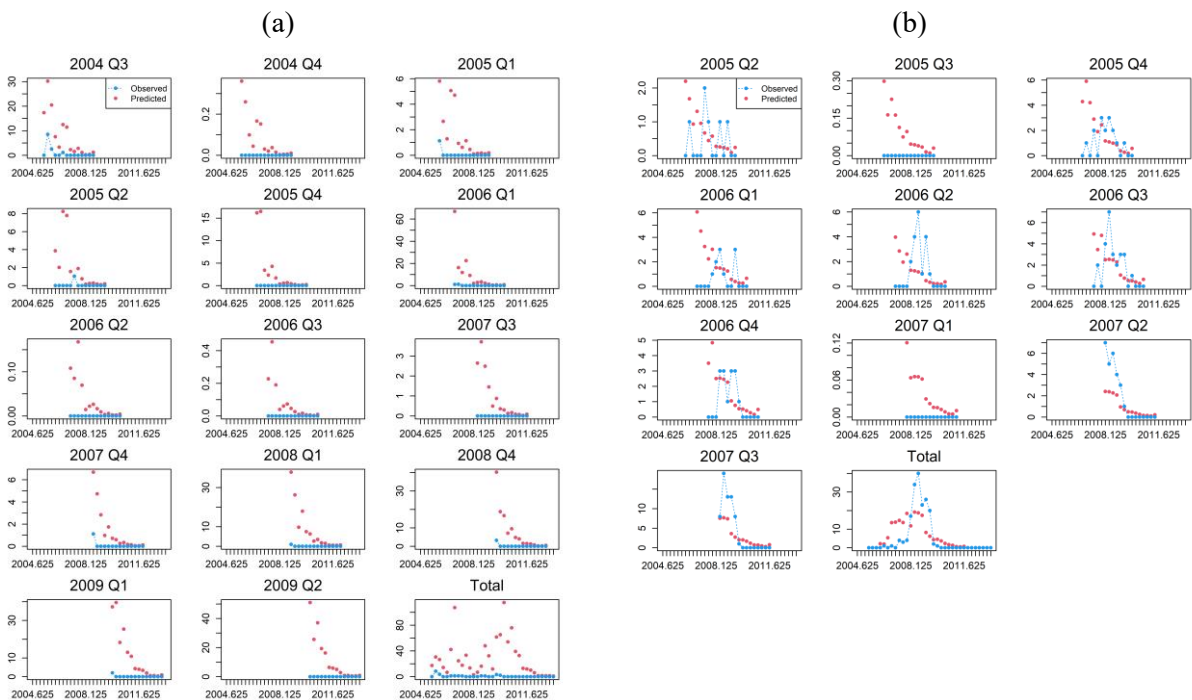


Figure B4: Observed and predicted the number of tag recoveries by quarter following the mixing period from the sensitivity model *rtss*: (a) recoveries of small-scale tags by the PSLS fishery, (b) recoveries of RTTP tags by the PL fishery. Tag release groups represent the total releases in each quarter.

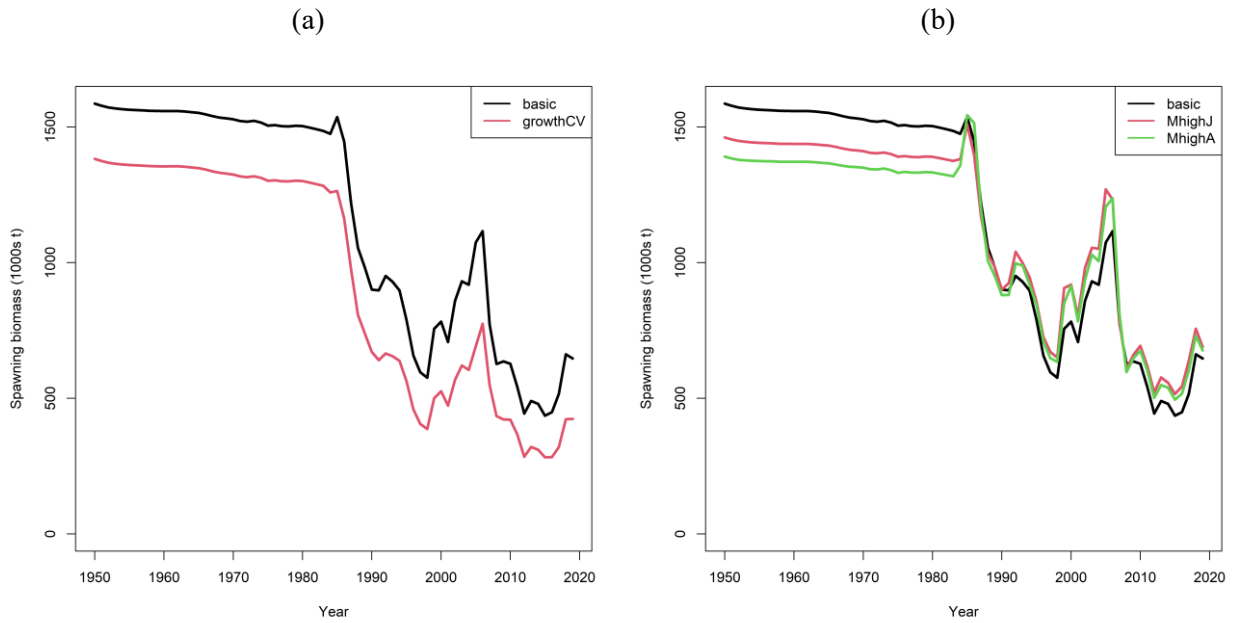


Figure B5: A comparison of estimated spawning biomass from sensitivity models related to biological parameter options – (a) model *growthCV* (b) model *MhighJ* and *MhighA*. A description of the sensitivity models is given in Table 4.

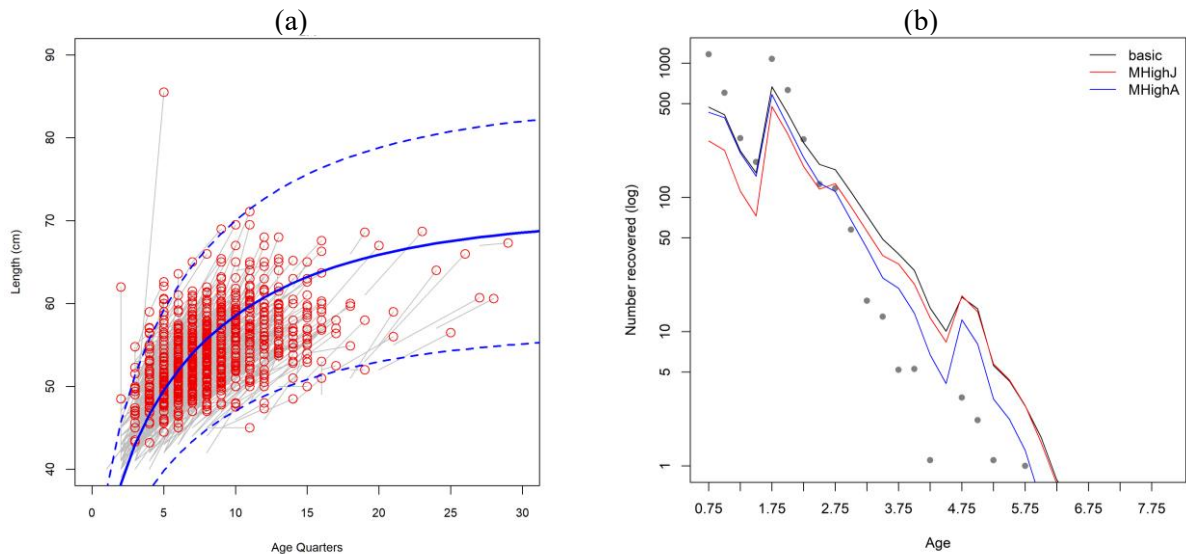


Figure B6: Diagnostics for sensitivity models related to biological parameter options – (a) a visual comparison of the basic growth variance option (a CV decreasing linearly from 20% at age 0 to 10% at maximum age), with tag-increments recovered from EU PS fleets, and (b) Observed (dots) and predicted number (on log scale) of tags recovered by age (aggregated for all fisheries) from *MhighJ*, *MhighA* and the basic model. Only tags at liberty after the three-quarter mixing period are included.

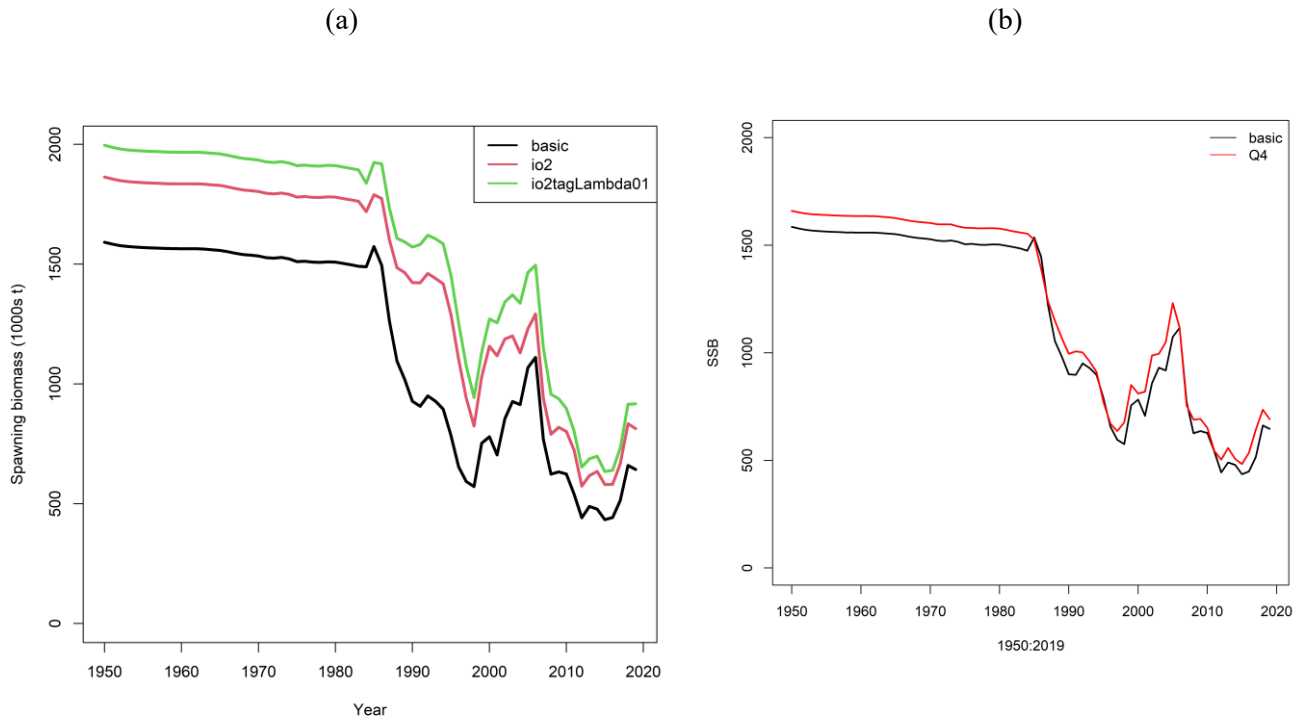


Figure B7: A comparison of estimated spawning biomass from sensitivity models related to (a) spatial structure, and (b) temporal structure. A description of the sensitivity models is given in Table 4.

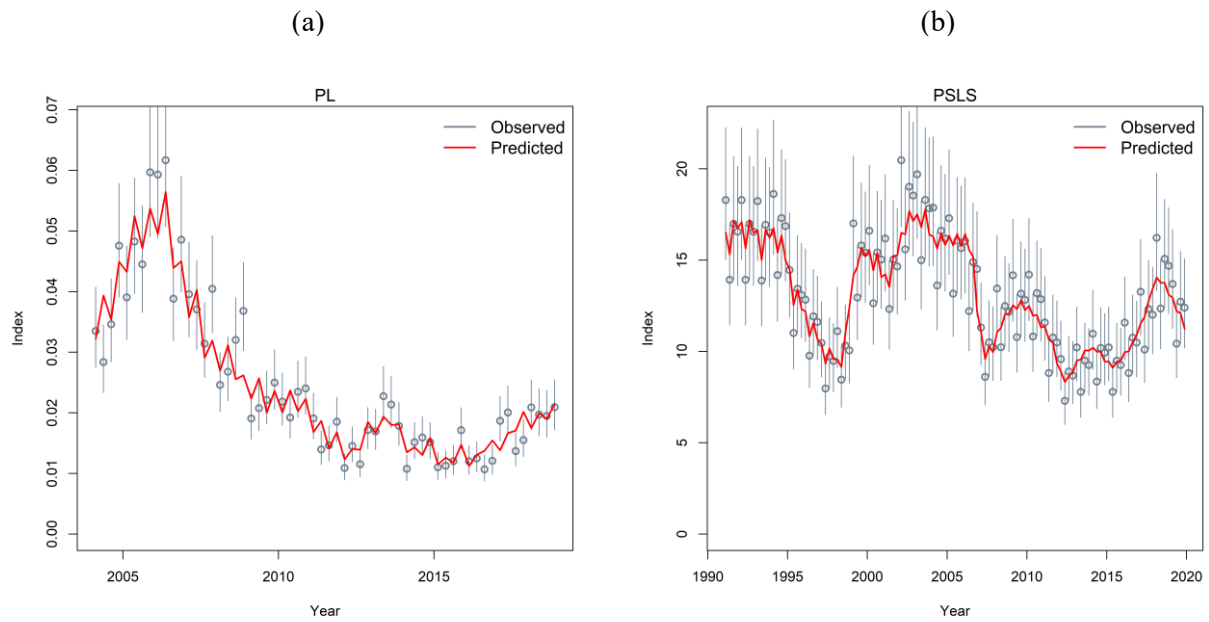


Figure B8: Fits to Maldives PL CPUE 2004 – 2018 and the EU PS CPUE 1991 – 2019 for the io2 model.

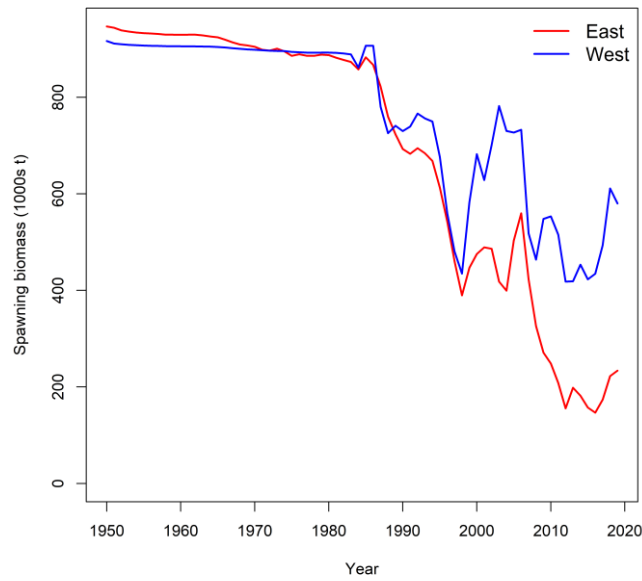


Figure B9: Estimates of regional spawning biomass for the two-area model io2.

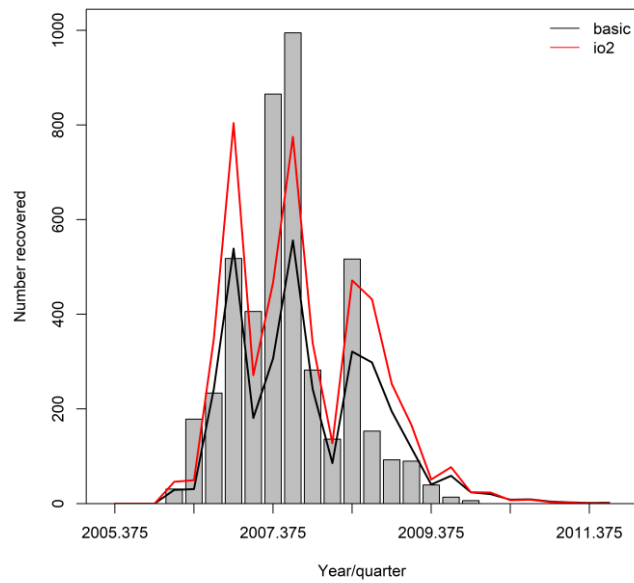


Figure B10: Observed (bars) and predicted number of tags recovered by year/quarter of recovery (aggregated for all fisheries) from io2, and the basic model. Only tags at liberty after the three-quarter mixing period are included.

APPENDIX C: RUN TEST RESULTS FROM THE TWO-AREA MODEL 'io2'

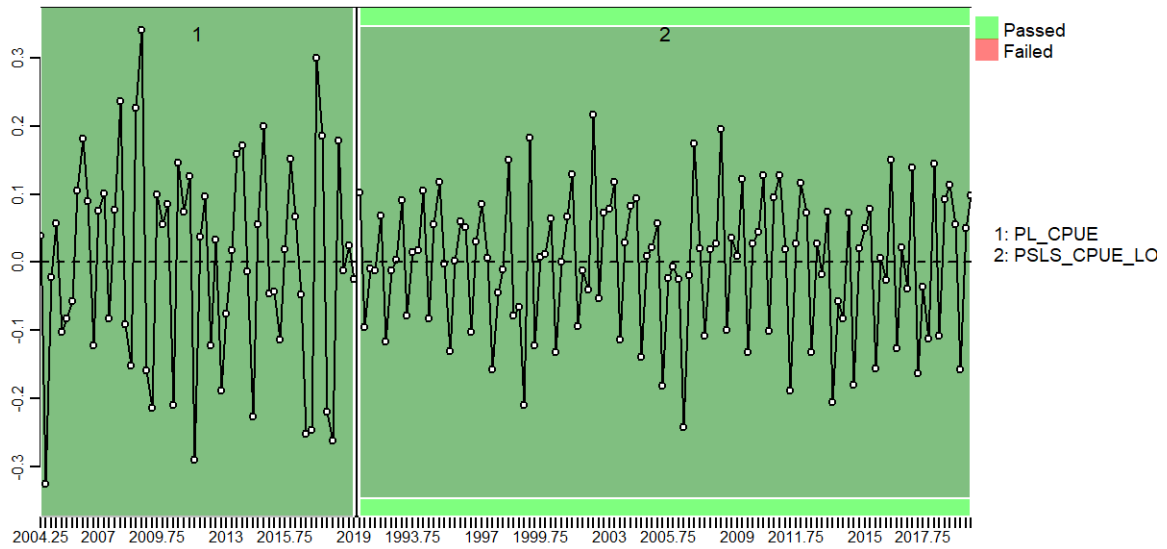


Figure C1: Runs tests performed to the time series of residuals from fits to PL and PSLs CPUE indices.

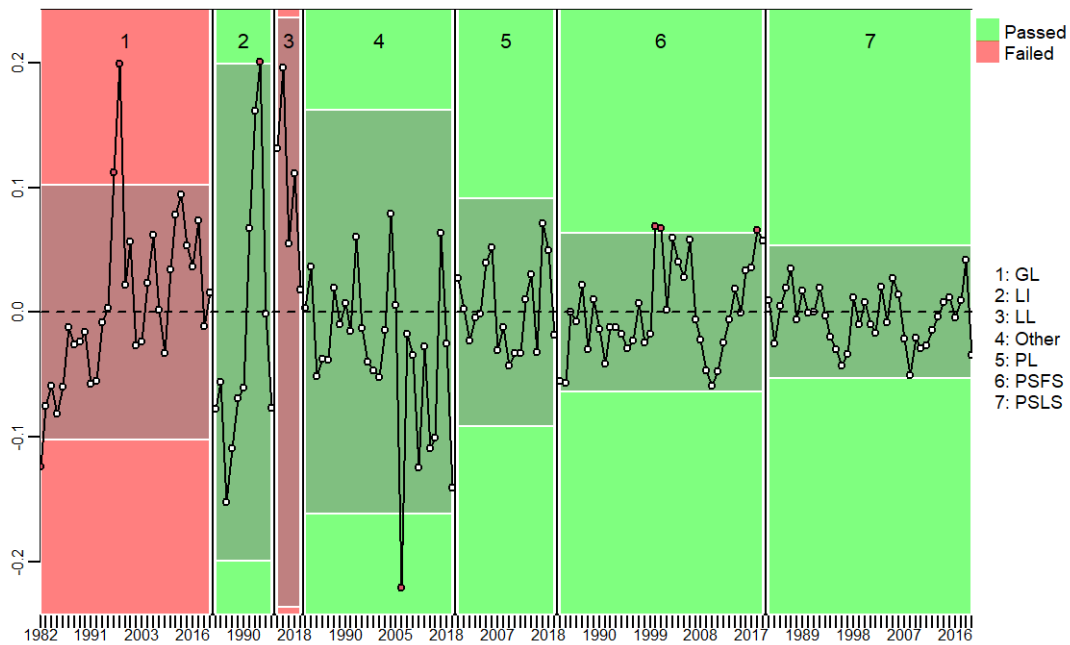


Figure C2: Runs tests performed to the timer series of residuals from fits to length composition data (by fishery).

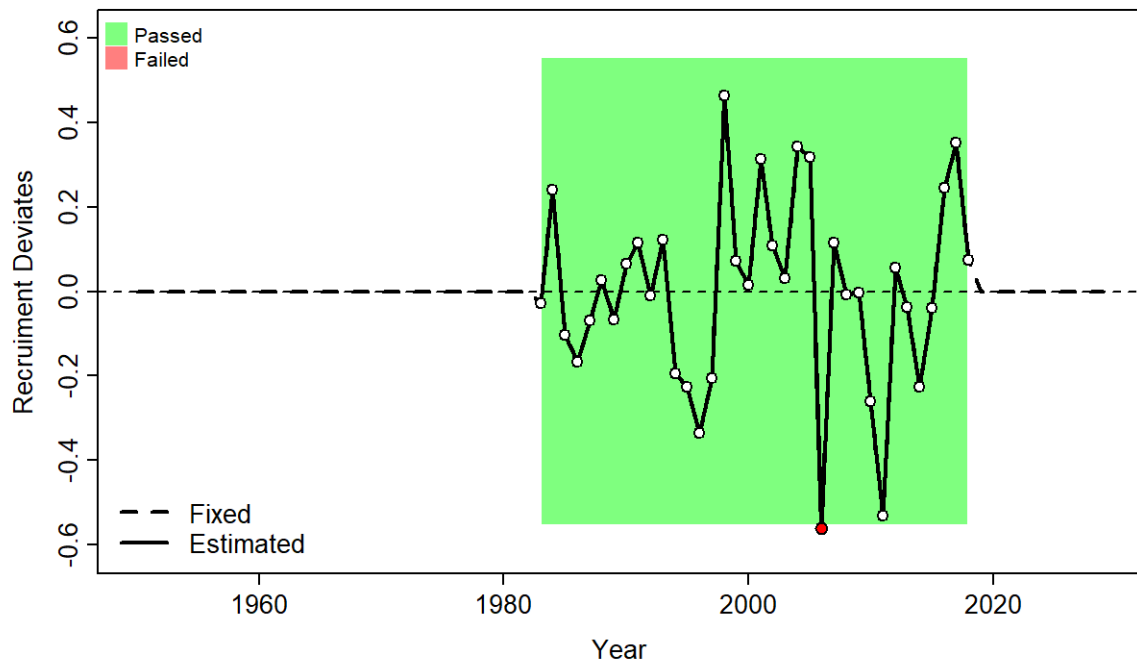


Figure C3: Runs tests performed to the timer series of recruitment deviates.